ACS OMEGA

Open Access

http://pubs.acs.org/journal/acsodf

Review

Review of Competitive Adsorption of CO_2/CH_4 in Shale: Implications for CO_2 Sequestration and Enhancing Shale Gas Recovery

Mengyao Cao, Chao Qin,* Yongdong Jiang, Peng Xia, and Ke Wang

Cite This: *ACS Omega* 2025, 10, 12756−12771

Read Online

ACCESS | Metrics & More | Article Recommendations

ABSTRACT: The injection of CO_2 into shale gas reservoirs can not only enhance shale gas recovery (ESGR), but also realize CO_2 geological storage (CGS). In this study, the competitive adsorption behaviors of CO_2 and CH_4 in shale were systematically reviewed, and the implication for shale gas recovery efficiency and CO_2 storage potential were discussed. The adsorption advantage of shale for CO_2 compared to CH_4 provides a guarantee of the feasibility of supercritical CO_2 ($ScCO_2$) enhanced shale gas exploitation technology. The selective adsorption coefficient of CO_2 and CH_4 by shale (S_{CO_2/CH_4}) is an important parameter in evaluating the competitive adsorption behavior of CO_2/CH_4 in shale gas reservoirs, which is closely related to the mineral composition, reservoir temperature, pressure conditions, water content, and mixed gas composition ratio. In addition, the injection type, injection mode, and injection rate of gases also exhibit different effects on CO_2/CH_4 competitive adsorption. Furthermore, the interaction between $ScCO_2$ and the water−rock system will change the mineral composition and microstructure of shale, which will lead to changes in the adsorption behavior of shale on CO_2 and CH_4, so its influence on the competitive adsorption of CO_2/CH_4 cannot be ignored. Future research should integrate different research methods and combine with practical engineering to reveal the competitive adsorption mechanism of CO_2/CH_4 in shale reservoirs from both micro and macro aspects. This study can provide support for the integration technology of $ScCO_2$ enhanced shale gas exploitation and its geological storage.

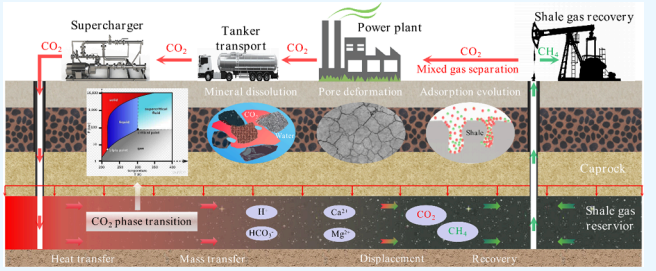

1. INTRODUCTION

Shale gas is a kind of unconventional natural gas, which mainly exists in adsorbed and free states in organic matter, clay minerals, and pore and fracture structures of shale, with the adsorbed gas accounting for 20−85% of the total gas content.[1] Hydraulic fracturing is one of the main technical means of shale gas exploitation, but the recovery rate of shale gas is generally low (<30%).[2] The typical curve of shale gas production over time is represented in Figure 1, and the gas production process of shale reservoirs can be divided into three stages, namely, the rapid decay stage (<400 days), the slow decrease stage (400−1000 days), and the stable development stage (>1000 days). A widely accepted explanation is that the free gas is mainly recovered in the early stage of shale gas production and the adsorbed gas is predominantly recovered in the later stage.[3,4] In view of the fact that adsorbed gas mainly exists in the nanoscale pores of shale, its recovery requires a greater driving force, which is one of the predominant reasons for the low gas production in the later stage of shale gas development.

Numerous studies[6−9] have indicated that the adsorption capacity of shale for CO_2 is significantly stronger than that of CH_4, thus the CO_2 huff-puff technology was suggested to be adopted in the later stage of shale gas development according to the shale oil reservoir development method. After injecting CO_2 into the shale gas reservoir, the CO_2 molecules will gradually enter the microscale or nanoscale pore structure along the fractured crack network and then exchange gas molecules with the residual adsorbed CH_4 in the form of competitive adsorption, which can promote the conversion of CH_4 from an adsorbed state to a free state, thereby improving the efficiency of shale gas recovery. Simultaneously, part of injected CO_2 will be captured by shale reservoirs to achieve CO_2 geological sequestration (Figure 2). Accordingly, the competitive adsorption behavior of CO_2/CH_4 after injecting CO_2 into the shale gas reservoir is a key factor affecting shale gas recovery and CO_2 storage.[9,10]

In order to realize the efficient development of shale gas and CO_2 geological storage, a large number of scholars have conducted a series of studies and achieved significant results. This study systematically reviews and summarizes the previous

Received: September 21, 2024
Revised: February 6, 2025
Accepted: February 12, 2025
Published: March 25, 2025

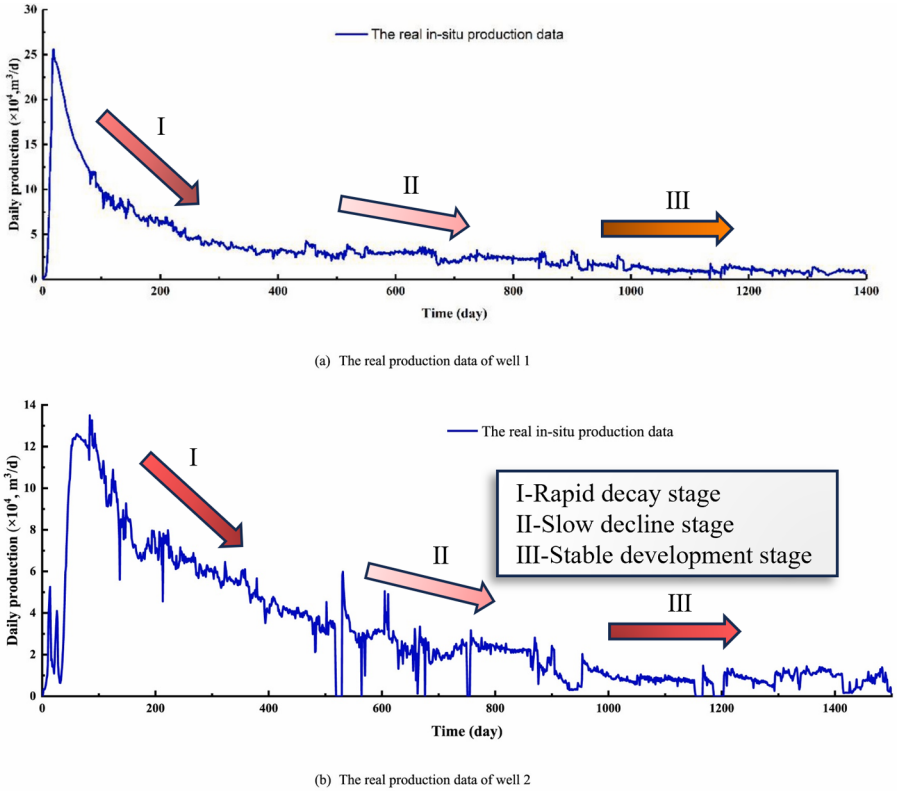

Figure 1. Actual production amount of shale gas wells.[5] (Photograph courtesy of Yang, R., copyright 2022, and the images in the figure are free domain.)

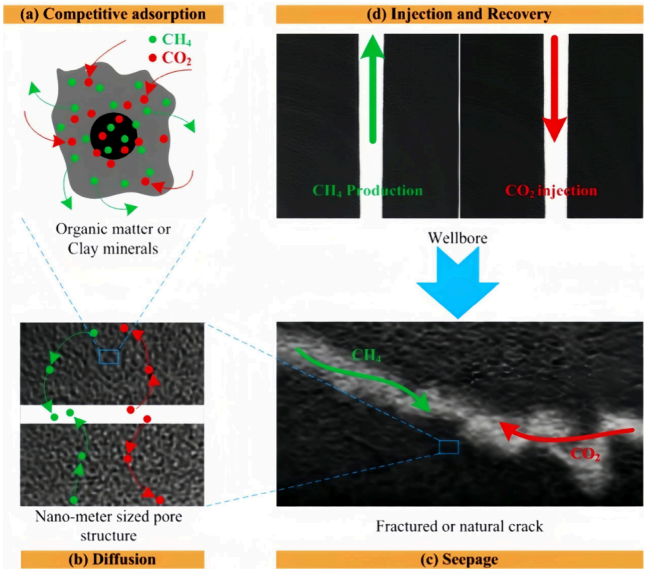

Figure 2. Schematic diagram of the integration of shale gas recovery and CO_2 geological storage.

research results, aiming to provide theoretical guidance for $ScCO_2$ enhanced shale gas exploitation technology. The targets and scope of this study include the following two parts:

(1) The effects of different factors on the competitive adsorption behavior of CO_2 and CH_4 in shale are reviewed and summarized, including the content and type of organic matter, mineral composition, reservoir temperature and pressure conditions, water content, mixed gas composition ratio, injection type, injection mode, injection rate, and $ScCO_2$−water−rock interaction.

(2) Based on the published relevant research, the shortcomings are pointed out, and then the directions of future attention and research are proposed.

2. CO_2/CH_4 COMPETITIVE ADSORPTION BEHAVIORS IN SHALE

After CO_2 is injected into shale gas reservoirs, CO_2 and CH_4 actually exist in the form of mixed gas. In view of the remarkable differences in the adsorption behavior of CO_2 and CH_4 in shale, the two kinds of gas molecules will compete for adsorption sites in the micro- or nanoscale pores of shale in the form of competitive adsorption, which will generate a certain impact on shale gas recovery and CO_2 geological storage. A large number of pure component gas adsorption experiments manifest that the thermodynamic parameters such as adsorption heat, Gibbs free energy, and entropy loss of CO_2 in shale are higher than those of CH_4; moreover, the adsorption capacity of CO_2 in shale is about 2−10 times that of CH_4.[11−13] It can be concluded that a greater adsorption advantage for CO_2 existed in shale rather than CH_4.[7,13,14] Accordingly, after CO_2 injection into the shale reservoir, CO_2 molecules will compete with adsorbed CH_4 molecules for adsorption sites due to the difference in the adsorption of CO_2 and CH_4 in shale, which indirectly promotes the desorption of CH_4 and improves the recovery rate of shale gas. Simultaneously, part of the injected CO_2 will be captured and stored in shale reservoirs. Currently, laboratory experiments, molecular simulations, and numerical analyses were principally used to investigate the competitive adsorption behavior of CO_2/CH_4 in shale.[7,15,16]

https://doi.org/10.1021/acsomega.4c08678
ACS Omega 2025, 10, 12756−12771

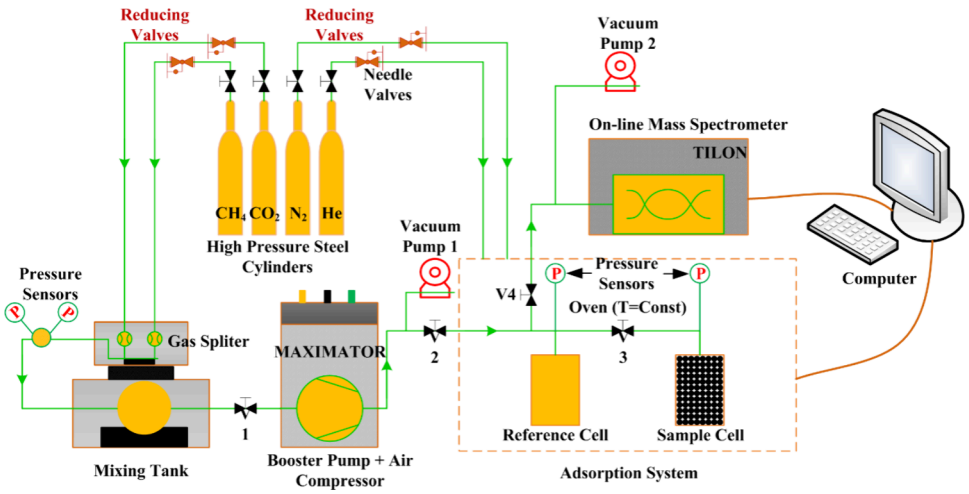

Figure 3. Mixed gas adsorption system.[15] (Photograph courtesy of Qin, C., copyright 2021, and the images in the figure are free domain.)

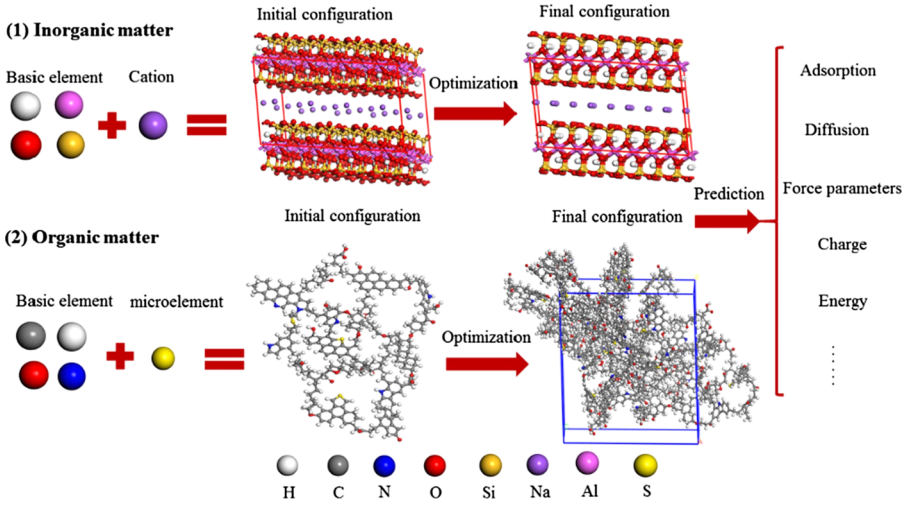

Figure 4. Construction method of a composite heterogeneous nanopore model containing organic matter and inorganic matter.[24] (Photograph courtesy of Ma, J., copyright 2022, and the images in the figure are free domain.)

2.1. Methods. *2.1.1. Laboratory Experiments.* The mixed gas adsorption test is the most direct and effective means to characterize the competitive adsorption characteristics of different gases in porous materials, while it is different from the pure component gas adsorption test due to the relatively complex experimental system, resulting in increased difficulty in the experiment. Figure 3 illustrates the typical mixed gas adsorption device.[15] It can be seen that the test device mainly consists of five parts: a gas mixing system, pressurization system, adsorption system, gas component calibration system, and computer control system. Compared with the pure component gas adsorption test, the main difficulties in the mixed gas adsorption test are as follows: 1) accurately configuring the composition ratio of the mixed gas; 2) accurately calculating the mixed gas adsorption capacity; and 3) obtaining kinetic adsorption data of mixed gases.

2.1.2. Molecular Dynamics Simulation. The difficulty with laboratory experiments is mainly reflected in the high accuracy requirements of experimental instruments, the complexity of the adsorption capacity calculation, and the challenge of analyzing various potential influencing factors. Thus, molecular simulation methods have gradually attracted the attention of scholars. Currently, density functional theory (DFT) based on quantum mechanics, the grand canonical Monte Carlo (GCMC) method based on statistical mechanics, and the molecular dynamics simulation (MD) based on Brownian motion are widely used.[17] According to the types of adsorbents, the corresponding inorganic matter models and organic matter models along with inorganic and organic compound models have been established.[18,19] Among them, the commonly used inorganic models mainly include quartz and clay minerals (montmorillonite, illite) models,[20] the organic models mainly include graphene nanomodels and kerogen models (mainly containing three types of kerogen: types I–III),[12,21,22] and the composite models use multilayer graphene structures.[23] Generally, the molecular simulation method can be used to conduct targeted research on different variables so as to obtain the influence of different potential factors (organic matter type, mineral composition, pore structure, temperature, pressure, water content, gas component ratio, etc.) on the competitive adsorption of multicomponent gases. Figure 4 shows the construction method of a composite heterogeneous nanopore model containing organic and inorganic matter.

2.1.3. Numerical Analysis. Currently, the numerical simulation software applied to the competitive adsorption of

https://doi.org/10.1021/acsomega.4c08678
ACS Omega 2025, 10, 12756−12771

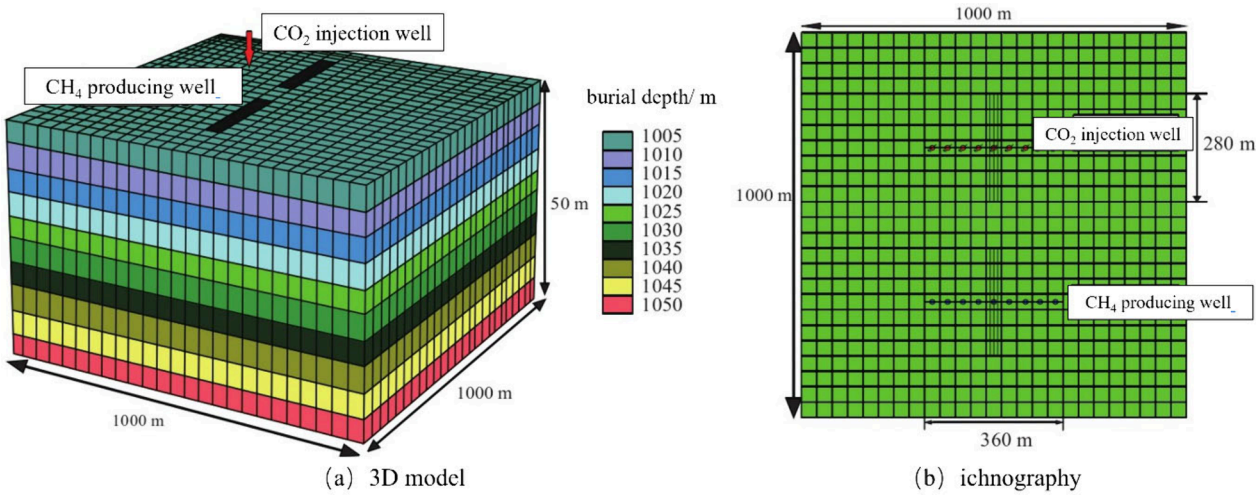

Figure 5. Schematic diagram of the double-porosity and double-permeability homogeneous model.[30]

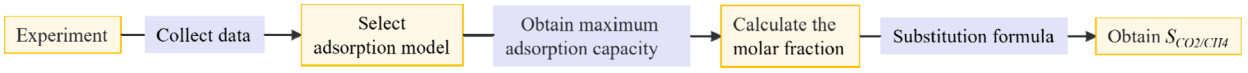

Figure 6. Calculation procedure of S_{CO_2/CH_4}.

Table 1. CO_2/CH_4 Competitive Adsorption Experiments of Different Shale Samples

References	Samples	Conditions	Main findings
Xie et al.[35]	Longmaxi	0−20 MPa 288−328 K	S_{CO_2/CH_4} decreases with the increases in CO_2 molar fraction, temperature, and pressure but is in direct proportion to TOC and clay mineral content.
Gu et al.[36,37]	Longmaxi Wufeng	0−2 MPa 278−318 K	S_{CO_2/CH_4} decreases with the increases in TOC, microporous content, and temperature but is inversely proportional to clay mineral content.
Qin et al.[15]	Yanchang	0−6 MPa 313 K	The molar fraction of CO_2 has no obvious effect on S_{CO_2/CH_4}. S_{CO_2/CH_4} gradually decreases with growing pressure; the $ScCO_2$−shale interaction resultes in a slight decline in S_{CO_2/CH_4}.
Liu et al.[9]	Longmaxi	0−10 MPa 303 K	S_{CO_2/CH_4} is proportional to the molar fraction of CO_2 and inversely proportional to the pressure.
Du et al.[38]	Wufeng	0−2 MPa 278−318 K	S_{CO_2/CH_4} enhances with the decreases in molar fraction of CO_2 and pressure, but the effect of temperature is not obvious.
Ortiz et al.[39]	Outcropping shale in the Iberian Range (Spain)	0−2 MPa --	S_{CO_2/CH_4} increases first and then decreases as the pressure grows.
Qi et al.[40]	Wufeng−Longmaxi	0−20 MPa 303 K/353 K	S_{CO_2/CH_4} is proportional to the molar fraction of CO_2 and temperature.
Liao et al.[6]	Wufen Longmaxi Yanchang	0−10 MPa 323 K	S_{CO_2/CH_4} increases first and then decreases with the molar fraction of CO_2; the variation with pressure is affected by the CO_2/CH_4 mixing ratio.
Ma et al.[41]	Longmaxi	0−15 MPa 323−363 K	The molar fraction of CO_2 in the mixed gas affects the trend of S_{CO_2/CH_4} with pressure.

multicomponent gases includes GEM, COMET, GCOMP, SIMED, and TOUGH2.[25−29] Taking GEM software as an example, by determining the mass equation, the relative permeability equation, and the adsorption equation, setting reservoir-related parameters (mineral composition, porosity, permeability, etc.) and initial conditions (initial pressure, temperature, water saturation, etc.), the migration process of CO_2 and CH_4 in the target geological body can be simulated to obtain the final CH_4 yield and CO_2 storage capacity so as to analyze the adsorption and displacement mechanism of CO_2 replacement for CH_4 in shale (Figure 5).

2.2. Influence Factors. A large number of competitive adsorption experiments of two-component and three-component gases on a coal matrix have been carried out and achieved remarkable results,[31,32] which have laid a theoretical foundation for studying the competitive adsorption characteristics of CO_2/CH_4 in shale. However, the adsorption capacity of shale for CO_2 and CH_4 is relatively weak compared to that of the coal matrix, and there are inevitable test errors in the mixed gas adsorption test, which makes it more difficult to conduct the multicomponent gas adsorption experiment in shale. According to the related report,[33] it can be found that the adsorption capacity of CO_2/CH_4 mixed gas in shale is between the values for pure CH_4 and pure CO_2 and displays an increasing trend with the increase in CO_2 concentration in the mixed gas. Based on the change in the molar fraction of each component in the free phase and the adsorbed phase of the mixed gas before and after adsorption, the selective adsorption coefficient can be used to evaluate the selective adsorption behavior of CO_2 and CH_4 in shale.[15] The calculation procedure is shown in Figure 6

$$S_{CO_2/CH_4} = \frac{x_{CO_2}/x_{CH_4}}{y_{CO_2}/y_{CH_4}} \quad (1)$$

https://doi.org/10.1021/acsomega.4c08678
ACS Omega 2025, 10, 12756−12771

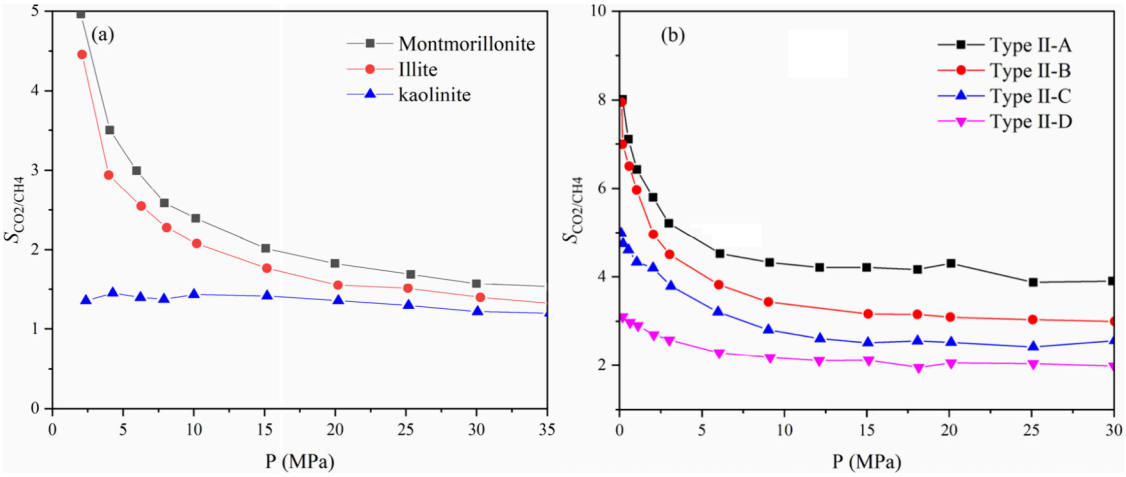

Figure 7. Effect of the types of clay minerals and organic matter on S_{CO_2/CH_4}. (a) Clay minerals;[48] (b) organic matter.[47] (Photograph courtesy of Hu, X., copyright 2019, and Sui, H., copyright 2020, and the images in the figure are free domain.).

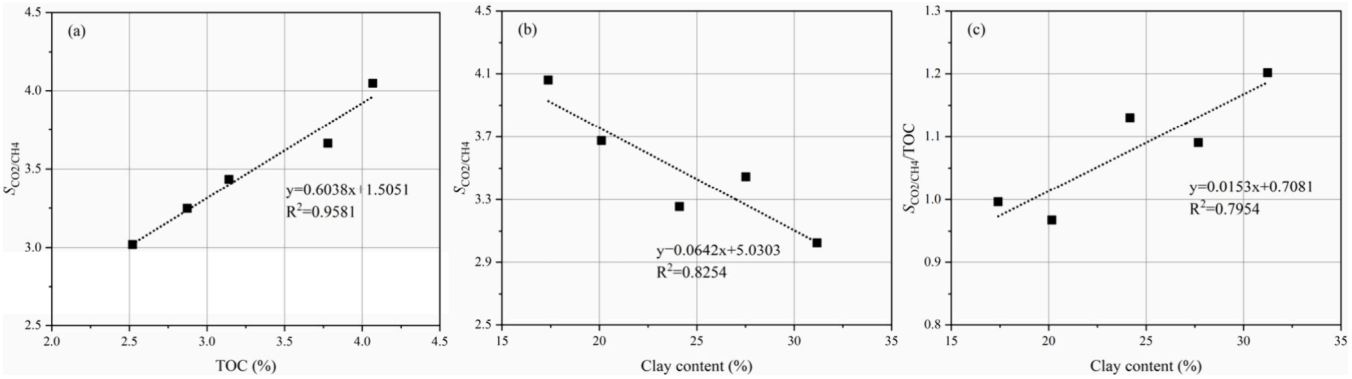

Figure 8. Relationship of S_{CO_2/CH_4} versus TOC and clay content.[35] (Photograph courtesy of Xie, W., copyright 2022, and the images in the figure are free domain.)

where S_{CO_2/CH_4} is the selective adsorption coefficient of CO_2 and CH_4 in shale (dimensionless), which is closely related to the properties of shale samples, water content, system temperature, and pressure; x_{CO_2} and x_{CH_4} represent the molar fractions of CO_2 and CH_4 in the adsorption phase (dimensionless); y_{CO_2} and y_{CH_4} represent the mole fractions of CO_2 and CH_4 in the free phase (dimensionless). Some scholars use local density to indicate the difference in the adsorption capacity of gases, and the local density represents the number of gas molecules in a specific region or location. Due to its large molecular size and strong polarity, CO_2 interacts more strongly and generally binds to the surface of porous materials (such as shale and coal) more readily than CH_4. As a result, CO_2 exhibits a larger local density and exhibits an adsorption capacity different from that of CH_4 molecules. Qi[34] uses the simplified local density theory (SLD) of multicomponent gases to calculate the actual local densities of different gases in the pores. The competitive adsorption capacity of CH_4 and CO_2 gases on the pore surface was obtained by comparing the local densities. The CO_2/CH_4 competitive adsorption experiments conducted in shale are represented in Table 1, which mainly involve the effects of the shale physical structure, reservoir conditions, and gas component ratio on S_{CO_2/CH_4}, and the following conclusions can be drawn.

2.2.1. Effect of Mineral Compositions. S_{CO_2/CH_4} is generally proportional to the content of TOC and inversely proportional to the clay mineral content. The effect of TOC on S_{CO_2/CH_4} is mainly related to the large number of micropore structures developed in shale organic matter.[42] An acceptable explanation is that the micropores belong to high-energy adsorption sites in shale, and the adsorption advantage of shale for CO_2 is particularly prominent in high-energy adsorption sites.[43] In addition, relevant scholars[44−47] have investigated the effect of organic matter type on the competitive adsorption behavior of CO_2 and CH_4 in shale, and the results indicated that the adsorption capacity and S_{CO_2/CH_4} of different kerogens are listed as follows: IA < IID < IIC < IIB < IIA < IIIA. (IA is typical of hydrogen-rich kerogen, II is deposited in marine environments, and IIIA is deposited in deltaic environments. The chemical formulas of kerogen types of II-A, II-B, II-C, and II-D are $C_{252}H_{294}O_{24}N_6S_3$, $C_{234}H_{263}O_{14}N_5S_2$, $C_{242}H_{219}O_{13}N_5S_2$, and $C_{175}H_{102}O_9N_4S_2$, respectively) (Figure 7 (b)). In addition, they found that the N groups, S groups, and O groups in kerogen exhibit a stronger adsorption capacity for CO_2. A similar conclusion obtained by Huang et al.[46] showed that CO_2 gas was preferentially adsorbed in the S groups in the kerogen of IA and IIA models and the N groups in the kerogen of IIIA models. The influence of clay minerals on S_{CO_2/CH_4} is also closely related to their mineral types, and

https://doi.org/10.1021/acsomega.4c08678
ACS Omega 2025, 10, 12756−12771

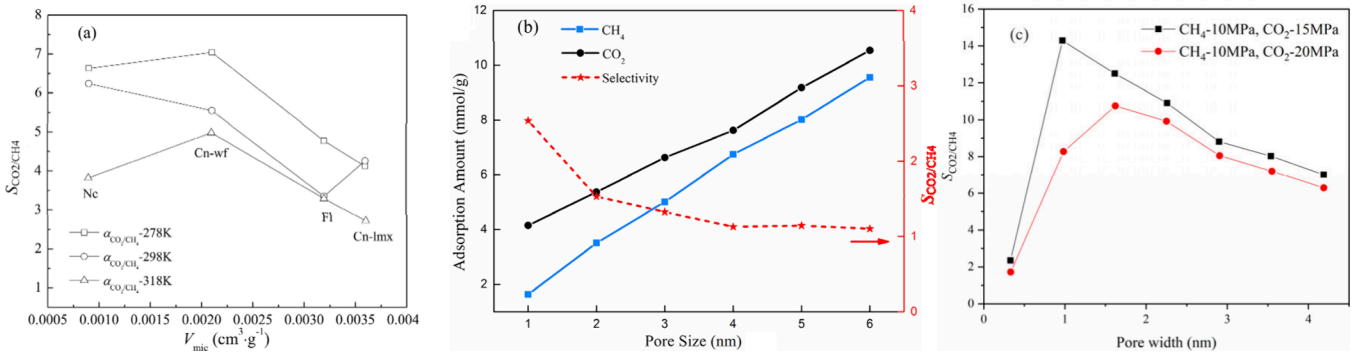

Figure 9. Effect of pore structure on S_{CO_2/CH_4}. (a) Shale samples,[37] (b) kaolinite,[50] and (c) organic matter.[51] (Photograph courtesy of Gu, M., copyright 2017, Zhou, W., copyright 2019, and Zhou, W., copyright 2018. The images in the figure are free domain.)

the orders of S_{CO_2/CH_4} for the clay minerals are montmorillonite > illite > kaolinite.[48] Specially, CO_2 molecules tend to occupy higher energy adsorption sites in montmorillonite and illite due to the cation exchange at low pressure, while a mixture of CO_2 and CH_4 begins to occupy the middle of the pore when the adsorption layer reaches saturation at higher pressures[46] (Figure 7 (a)).

It is worth noting that although S_{CO_2/CH_4} is negatively correlated with the content of clay minerals, it exhibits a positive correlation with the content of clay minerals after standardizing clay minerals with TOC (Figure 8), indicating that the influence of TOC on S_{CO_2/CH_4} may weaken the effects of clay minerals. The competitive adsorption behavior of CO_2 and CH_4 in clay minerals is not only related to its internal pore structure but also affected by its hydrophilic properties.[49] Water molecules will occupy part of the adsorption sites in clay minerals, thus affecting the adsorption behavior of CO_2 and CH_4. Therefore, it is necessary to consider the potential influence of hydrophilic properties on the competitive adsorption behavior of CO_2 and CH_4 in clay minerals. Through molecular simulation studies, Hu et al.[48] found that although cation exchange sites are mostly in clay minerals, the 1:1 layer structure of kaolinite lacks the interlayer space necessary for cation accommodation and exchange, coupled with the strong internal bonding and lack of charge-balancing requirements, so it does not have cation exchange. Cations may alter the adsorption sites' energy landscape and significantly improve S_{CO_2/CH_4}; therefore, the selective adsorption capacity of kaolinite is not as good as that of montmorillonite and illite. Additionally, they consider that the charge effect may be the main factor that leads to a stronger adsorption capacity of CO_2 than CH_4 in clay minerals. Specifically, the presence of exchangeable cations will affect the ionic strength of shale pore water and the charge distribution on the shale surface, enhancing the solubility of CO_2 in the water phase. In addition, due to the different polarization properties of CO_2 and CH_4, the electrostatic interaction between CO_2 molecules and the shale surface is stronger than that of CH_4, so it is easier to adsorb.

2.2.2. Effects of Pore Size and Content. Aiming at the influence of micropores, Duan et al.[36] and Xie et al.[35] denoted that S_{CO_2/CH_4} was directly proportional to the micropore content through experiments, while an unobvious correlation between micropore content and S_{CO_2/CH_4} was represented in the study of Gu et al.[37] A possible interpretation is that the micropores obtained in the study of Gu et al.[37] are not the real micropore content of shale (the low-temperature N_2 adsorption method was used to measure the pore structure of shale in their study, while this method can test pores only above 1.5 nm). In addition, molecular simulation has been used to study the effect of different pore size ranges on the competitive adsorption of CO_2 and CH_4. Zhou et al.[50] indicated that S_{CO_2/CH_4} decrease with the increase in pore size based on the model of kaolinite clay minerals, while a different result was obtained according to a graphene slit model of organic nanopores in shale.[51] They[51] discovered that S_{CO_2/CH_4} first increased and then decreased in the pore size range of 1.0−4.0 nm, and there was a maximum value of around 1.5−2.0 nm (Figure 9). Furthermore, Qi et al.[52] denoted that 0.42 nm is the critical size that determines which gas in CO_2 and CH_4 is preferentially adsorbed, and CH_4 will be preferentially adsorbed when the pore size is less than 0.42 nm; otherwise, CO_2 will be preferentially adsorbed. The possible explanations for this phenomenon are as follows: The pore wall exhibits a repulsive effect on gas molecules, and the repulsive effect on CO_2 in smaller pores (≤0.42 nm) is greater than that of CH_4, resulting in a weakened adsorption capacity for CO_2. The CO_2 molecule (carbon dioxide) is smaller than the CH_4 molecule (methane) and has a linear structure, whereas the CH_4 molecule is spherical. Thus, smaller CO_2 molecules are more likely to enter smaller nanopores. In addition, due to the interaction of the pore wall, the adsorption capacity of the gas molecules will be enhanced, and smaller CO_2 molecules can adapt to the pore geometry more easily and form stronger adsorption on the pore wall. In nanopores, the van der Waals forces between the gas molecules and the pore wall have a significant effect on the adsorption. Finally, because CO_2 molecules have stronger polarity and higher dipole moments, the van der Waals forces between CO_2 molecules and the pore wall are stronger than those for CH_4 molecules. In smaller pores, the diffusion rate of gas molecules is limited, while smaller CO_2 molecules diffuse at a faster rate than CH_4 molecules, which makes it easier for them to diffuse through pores and occupy adsorption sites.[52]

It is worth mentioning that the variations of pore size can affect the adsorption behavior of CO_2 and CH_4 in shale. Related studies[53−55] have demonstrated that CO_2 and CH_4 are mainly adsorbed in the form of micropore filling in micropores, while they are mainly adsorbed in the form of monolayers in mesopores and macropores. This is a topic of constant debate regarding whether the gas adsorption mechanism in shale is

https://doi.org/10.1021/acsomega.4c08678
ACS Omega 2025, 10, 12756−12771

monolayer adsorption or micropore filling. Zhou et al.[50] pointed out that the strong adsorption layer is mainly due to the monolayer adsorption mechanism, while the weak adsorption layer is caused by micropore filling. Their research shows that in micropores, gas molecules first form a single layer of adsorption (strong adsorption layer) on the pore wall, and as the pressure increases or the pore diameter decreases, gas molecules begin to fill in the pores to form weak adsorption layers. The change in pore size (1−6 nm) has no obvious effect on monolayer adsorption but has a great effect on micropore filling adsorption. With the increase in pore size, the effect of micropore filling adsorption gradually weakens, and when the pore size is larger than 2 nm, the effect can be ignored (Figure 10). This may be related to factors such as gas pressure,

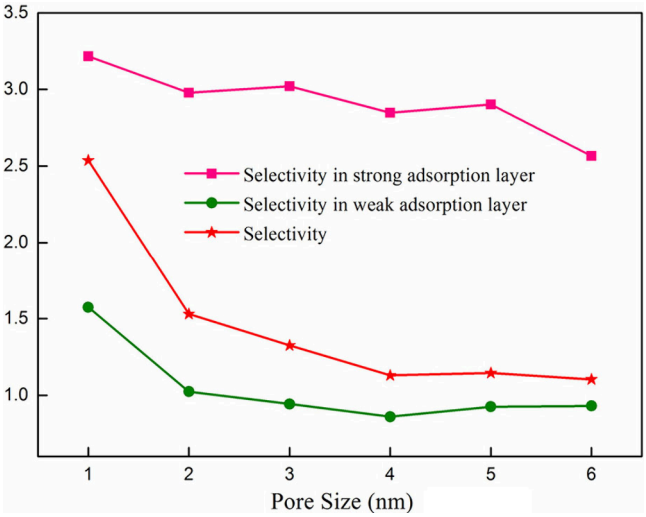

Figure 10. Selectivities in different adsorption layers.[50] (Photograph courtesy of Zhou, W., copyright 2019, and the image in the figure is free domain.)

temperature, fluid density, and pore size. Under high-pressure conditions, gas molecules are more inclined to form multilayer adsorption in the pores and the increase in temperature will reduce the density of gas molecules in the adsorption layer, so low temperature is conducive to gas adsorption. In addition, the increase in pore size will weaken the adsorption affinity of the pore structure to gas molecules, thus reducing the adsorption capacity of gas molecules. A similar conclusion was obtained by Zeng et al.,[56] and they manifested that the increase in pore size would weaken the adsorption affinity of the pore structure to gas molecules, thus reducing the number of adsorbed gas molecules. It should be noted that the development of pore fracture structure in shale is closely correlated with the diversity of mineral species, but the effect of the pore structure of different minerals on the S_{CO_2/CH_4} has received little attention.

2.2.3. Effect of Reservoir Temperature and Pressure Conditions. S_{CO_2/CH_4} is inversely proportional to the system temperature, but the influence of the system pressure remains to be further studied. Regarding the influence of temperature, although the adsorption capacity of shale for CO_2 and CH_4 decreases with increasing temperature,[57] the degree of decrease in CO_2 adsorption is higher than that of CH_4 due to the critical temperature of CO_2 being higher than that of CH_4, resulting in a decreasing trend of S_{CO_2/CH_4} with increasing temperature. The conjecture can be verified by the research results in Figure 11. And Bai[58] studied the adsorption behavior of CO_2 molecules under subcritical and supercritical temperatures and found that the change law of gas adsorption-phase properties was determined by the special properties of near-critical fluid and the pore structure of adsorbent. Below the critical temperature, because the adsorption energy of gas molecules is usually lower than the thermal energy in the body phase, they are inclined to be adsorbed. However, as the temperature approaches or exceeds the critical temperature, the thermal energy increases, the interaction of gas molecules is weakened, and the active sites on the surface of the adsorbent are saturated faster, which may lead to the desorption of gas and reduce the adsorption amount. In addition, when the critical temperature is exceeded, the pores may expand or contract, affecting the accessibility of the pores and the availability of adsorption sites. Due to the high critical temperature of CO_2, there are differences between CO_2 and CH_4 in the adsorption process in terms of intermolecular force and adsorption heat, so its adsorption behavior is more sensitive when it is close to the critical temperature. The adsorption heat of CO_2 is usually higher than that of CH_4, so more heat is released during the adsorption process. At higher temperatures, the thermal movement of the CO_2 molecules is intensified, so they will be easier to desorb from the adsorbent surface.

In view of the influence of pressure, relevant scholars[7,50] found that S_{CO_2/CH_4} decreased with increasing adsorption pressure through laboratory tests, and they indicated that the gas molecules will be preferentially adsorbed at the high-energy adsorption site of kerogen under low-pressure conditions. In this case, the interactions between kerogen and gas molecules is dominant, and the adsorption advantage of CO_2 is reflected.[60] As the pressure increases, the high-energy adsorption sites are gradually occupied, and the gas molecules can compete for only the adsorption sites on the low-energy adsorption sites. In this case, the interaction force of the gas molecules is dominant, thus resulting in the weakening of the adsorption advantage of CO_2, and S_{CO_2/CH_4} gradually tends to be balanced.[47] However, different results were discovered by Liao et al.[6] and Ortiz et al.[39] They discovered that the S_{CO_2/CH_4} of some shale samples increased first and then decreased with increasing pressure (Figure 12). A possible explanation is that the TOC and clay mineral (illite) content of the tested samples are relatively high, resulting in the adsorption capacity of the high-energy adsorption site in shale not reaching the saturation state under low-pressure conditions. In addition, the gas injection volume will increase with increasing pressure, while the adsorption capacity of CO_2/CH_4 in shale in the whole adsorption system is limited, which can lead to the increase of residual gas. Therefore, the influence of the free phase ratio on S_{CO_2/CH_4} will be weakened according to eq 1; namely, the y_{CO_2}/y_{CH_4} will gradually approach the original gas injection ratio with the increase in gas injection, thus resulting in the decrease in S_{CO_2/CH_4}.

2.2.4. Effect of Water Content. The variation of S_{CO_2/CH_4} with water content is closely related to the type of organic matter in shale. Huang et al.[61] indicated that the S_{CO_2/CH_4} of the kerogen of IIA, IIC, and IID increased with increasing water content while that of kerogen with IIB decreased with

https://doi.org/10.1021/acsomega.4c08678
ACS Omega 2025, 10, 12756−12771

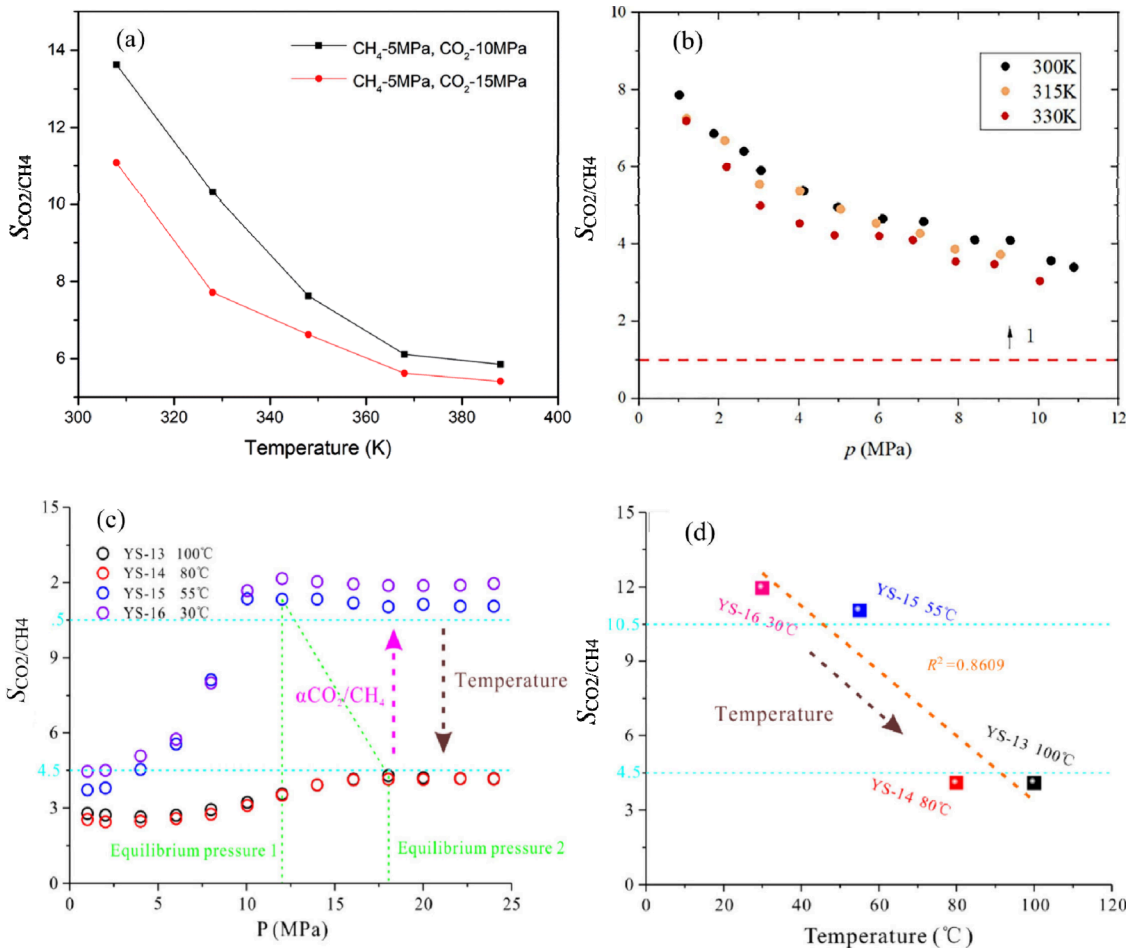

Figure 11. Effect of pressure (MPa) and temperature (K for (a) and (b),°C for (c) and (d)) on S_{CO_2/CH_4}. (a) Shale organic nanopores,[51] (b) shale of the Longmaxi Formation,[59] (c) shale of the Longmaxi Formation,[54] and (d) shale of the Longmaxi Formation.[54] (Photograph courtesy of Zhou, W., copyright 2018, Lu, T., copyright 2022, and Xie, W., copyright 2021. The images in the figure are free domain.)

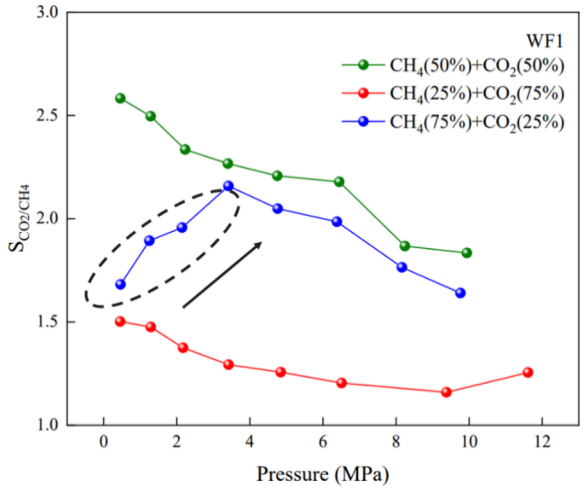

Figure 12. Change in S_{CO_2/CH_4} with adsorption pressure in shale.[6] (Photograph courtesy of Liao, Q., copyright 2023, and the image in the figure is free domain.)

increasing water content when the pressure is >3 MPa (Figure 13). In addition, the distribution of water molecules in kerogen varies significantly under different water content conditions. Relevant scholars[46,47,62] denoted that the water molecules will be irregularly dispersed in kerogen pores and mainly exist on the pore surface in the form of water film under the condition of low water content while most of the water molecules will form clusters and distribute in the pore center under the condition of high water content, which will lead to the pore space of kerogen being occupied by a large number of water molecules, thus reducing the adsorption capacity of kerogen for CO_2 and CH_4. On this basis, Zhou et al.[50] indicated that the polarity of water molecules is stronger than that of CO_2 and CH_4 molecules, which is the main reason that water molecules are more likely to occupy the adsorption site of kerogen. Simultaneously, the water molecules also tend to adsorb to each other and form clusters on hydrophilic clay minerals, which will further interfere with the adsorption of the CO_2 and CH_4 molecules. Furthermore, it is worth emphasizing that the molar ratio of mixed gas will change the variation of S_{CO_2/CH_4} with the water content. Zhang et al.[63] discovered that the S_{CO_2/CH_4} in kerogen decreased sharply with the increase in water content when the molar fraction of CO_2 is high while it increased with increasing water content when the molar fraction of CH_4 is high.

2.2.5. Effect of the Proportion of Each Component in the Mixed Gas. The effect of the variation of the CO_2 molar fraction on S_{CO_2/CH_4} remains to be further studied. With the increase in the CO_2 molar fraction in the CO_2/CH_4 gas

https://doi.org/10.1021/acsomega.4c08678
ACS Omega 2025, 10, 12756−12771

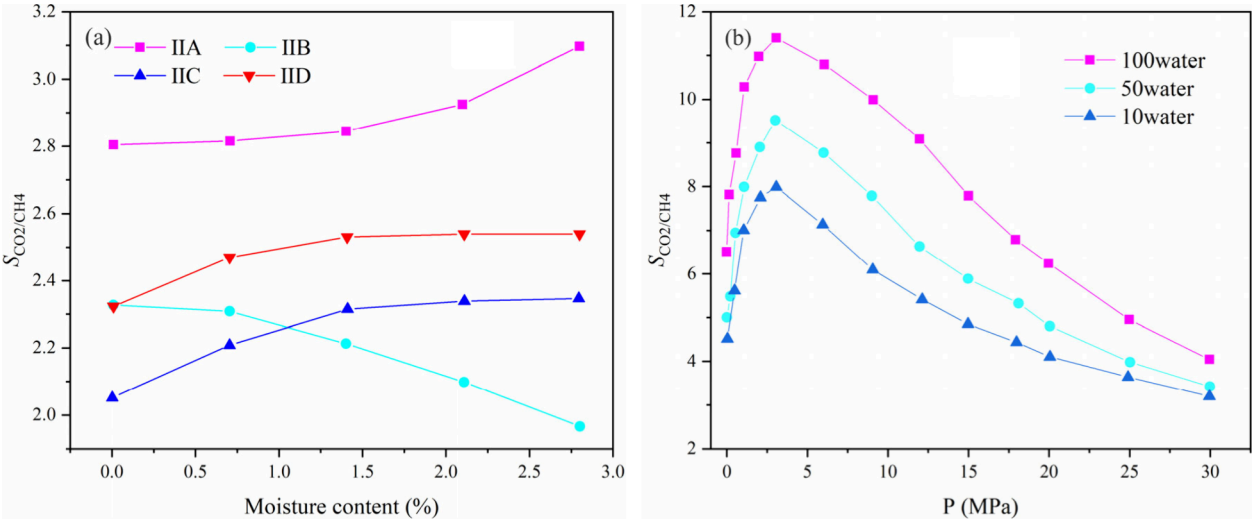

Figure 13. Effect of the water content on S_{CO_2/CH_4}. (a) Different kerogen models;[61] (b) type II-D kerogens (10 water, 50 water, and 100 water mean 10, 50, and 100 water molecules).[47] (Photograph courtesy of Huang, L., copyright 2018, and Sui, H., copyright 2020, and the images in the figure are free domain.).

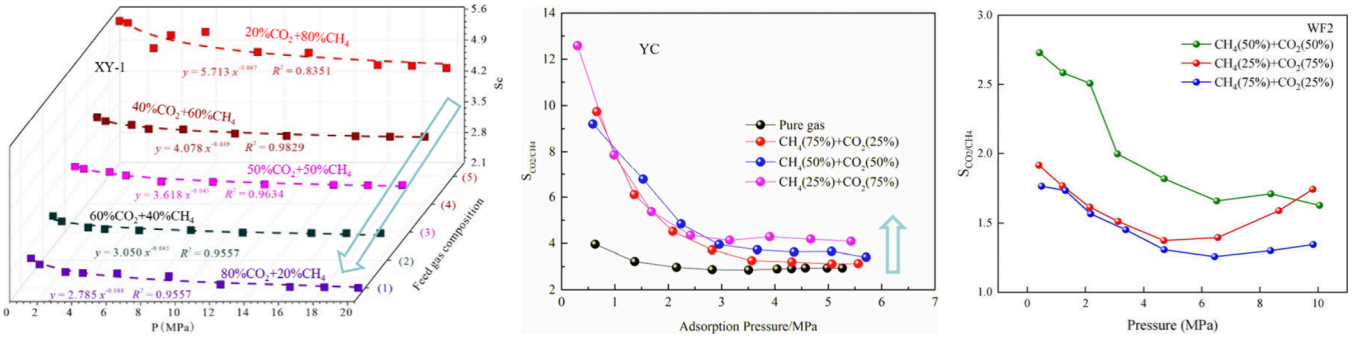

Figure 14. Effect of the mixing ratio of CO_2/CH_4 on S_{CO_2/CH_4}.[6,15,35] (Photograph courtesy of Liao, Q., copyright 2023, Qin, C., copyright 2021, and Xie, W., copyright 2022, and the images in the figure are free domain.)

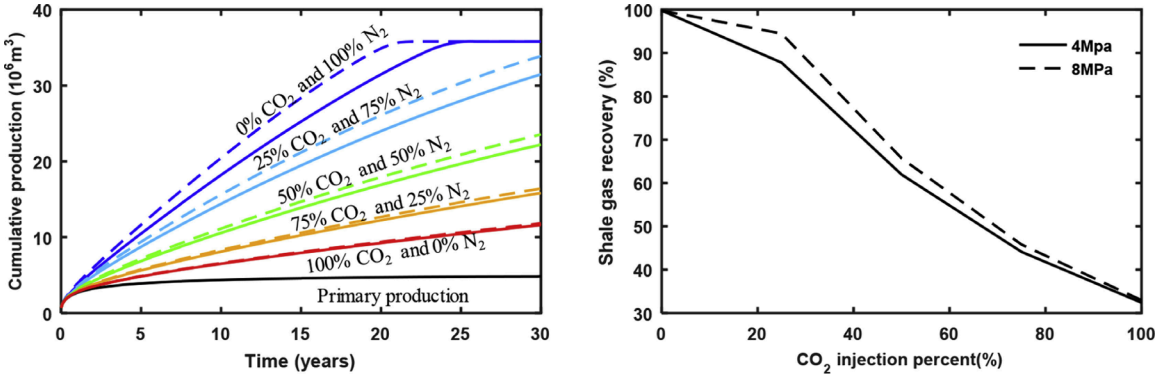

Figure 15. Effects of different CO_2/N_2 injection ratio on recovery efficiency of shale gas (solid lines mean <4 MPa overpressure injection and dashed lines mean <8 MPa overpressure).[65] (Photograph courtesy of Li, Z., copyright 2019, and the image in the figure is free domain.)

mixture, S_{CO_2/CH_4} exhibited a decreasing trend reported by Xie et al.[35] while it displayed a slightly increasing trend published by Qin et al.[15] In addition, Liao et al.[6] discovered that the S_{CO_2/CH_4} obtained by the mixing ratio of 50%:50% was significantly higher than that of other mixing ratios (Figure 14). It is pointed out that the variation of S_{CO_2/CH_4} with the proportion of mixed gas components may be related to the difference in molecular properties of different gases and the adsorption affinity of different adsorption sites in shale for gas molecules.[50,64] However, this inference is only given a qualitative description and lacks a sufficient explanation at present. Consequently, it is necessary to explore the interaction relationship of different gas molecules in shale from the molecular level, thereby providing a theoretical reference for the influence mechanism of the gas mixing ratio.

2.2.6. Effect of the Injection Gas. In addition to injecting CO_2 gas into shale reservoirs, the injection of N_2 or a mixture

https://doi.org/10.1021/acsomega.4c08678
ACS Omega 2025, 10, 12756−12771

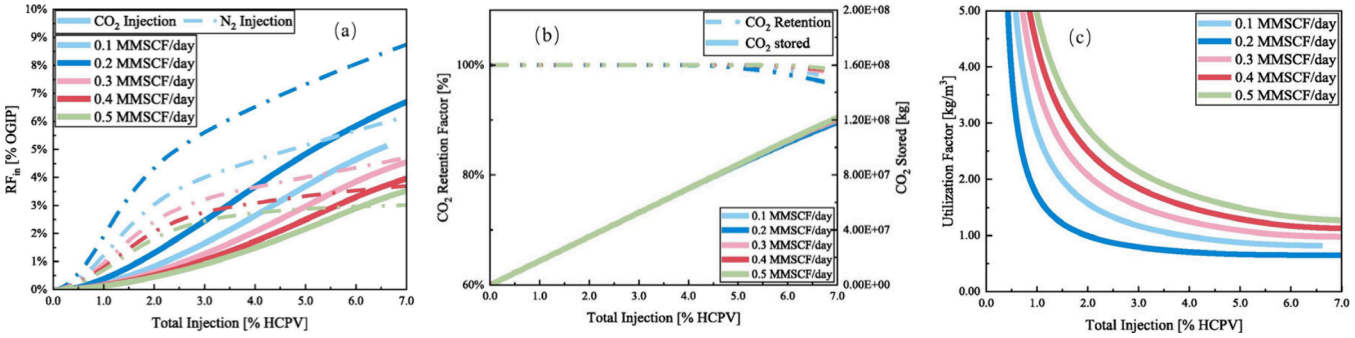

Figure 16. Effects of changes in CO_2 and N_2 injection rates on gas recovery and CO_2 storage.[67] (Photograph courtesy of Ma, H., copyright 2022, and the image in the figure is free domain.)

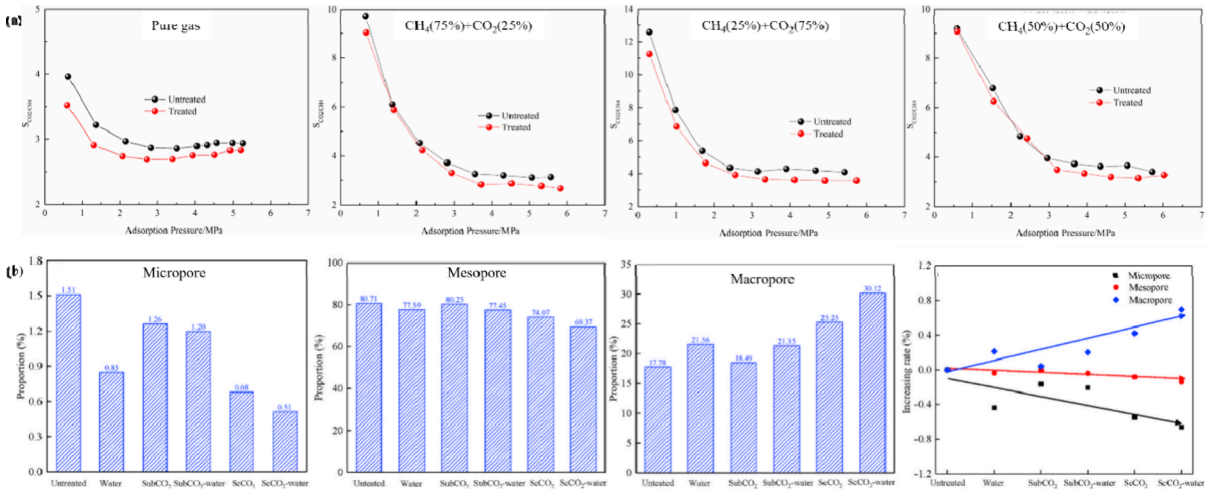

Figure 17. Effect of $ScCO_2$ immersion on S_{CO_2/CH_4} and pore structure of shale.[15,74] (Photograph courtesy of Qin, C., copyright 2021, and Zhou, J., copyright 2021, and the images in the figure are free domain.)

of N_2 and CO_2 can also improve the recovery rate of shale gas to a certain extent, while significant differences existed in the replacement mechanism of the two injected gases. Related studies through experiments and simulations[65−68] have indicated that both CO_2 and N_2 injection can improve the recovery rate of shale gas to a certain extent (2−80%), but the injection effects of the two schemes are significantly different (Figure 15). They demonstrated that the injection effect of N_2 for shale gas recovery is obviously better than that of CO_2, which is mainly due to the fact that the injection of N_2 can promote the desorption of CH_4 by reducing the partial pressure of CH_4, and this effect is stronger than the influence of CO_2/CH_4 competitive adsorption on shale gas recovery. Accordingly, it is recommended to inject a mixed gas of CO_2 and N_2 into the shale reservoir in practical engineering projects, which can not only improve shale gas recovery but also achieve CO_2 geological storage. However, how to choose the appropriate injection ratio of CO_2 and N_2 is a problem worthy of attention, which may be related to the geological conditions, physical parameters, and construction technology of shale reservoirs and should be paid attention to in future practical projects.

2.2.7. Effect of the Injection Mode and Injection Rate. Li et al.[69] used a reservoir simulation model of multicomponent transport in dual porosity sorbing and swelling media to compare different injection modes, and they found that compared with the continuous injection of CO_2 into shale reservoirs for improving shale gas recovery, the effect of huff and puff injection is more significant. In addition, the effectiveness of ESGR and CGS can be affected by the injection rate, and the increase of the gas injection rate is beneficial to ESGR and CGS when the injection rate is low while an opposite effect existed when the injection rate exceeds a certain threshold (Figure 16). Consequently, a reasonable gas injection rate should be selected according to the actual shale reservoir conditions.

As can be seen from Figure 16, the increase in the injection rate can improve the recovery rate of shale gas before fracture breakthrough, and the main reason is that the permeability of the fracture cannot be effectively improved when the gas injection rate is low, thus leading to CH_4 molecules that cannot flow out. However, there is a threshold for the injection rate, and the shale gas recovery rate will decrease as the injection rate increases when the injection rate exceeds this threshold (Figure 16 (a) dark blue curve, 0.2 MMSCF/day, MMSCF is a measure of the natural gas volume and stands for million standard cubic feet). A possible interpretation is that the fracture breakthrough time may be shortened after exceeding the injection rate threshold and it is difficult to extract natural gas because the fracture permeability is not effectively improved. In addition, it can be seen from Figure 16 (b) that the injected CO_2 can be successfully sealed as long as the breakthrough point is not reached. Although more CH_4 can be recovered with the increase in the gas injection rate, the

https://doi.org/10.1021/acsomega.4c08678
ACS Omega 2025, 10, 12756−12771

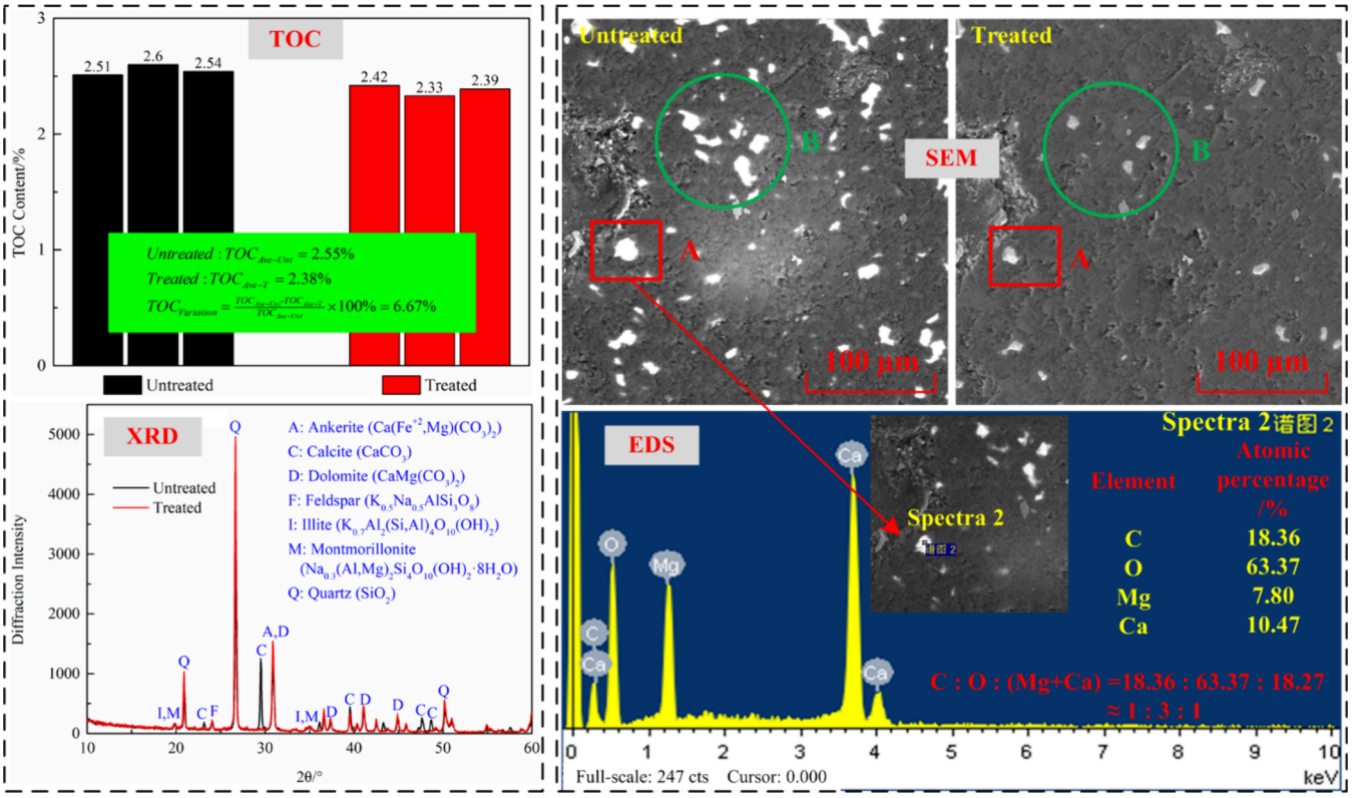

Figure 18. Variations in shale mineral composition before and after $ScCO_2$ exposure.[76]

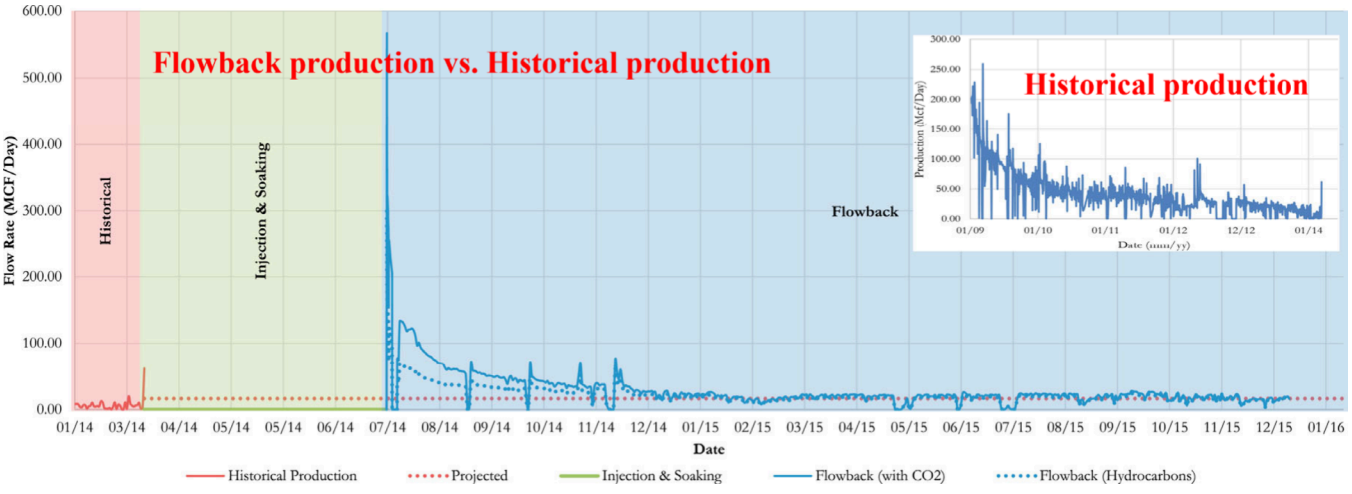

Figure 19. CO_2-ESGR project in the Chachattooga shale reservoir.[10] (Copyright 2017 and the image in the figure is free domain.)

utilization efficiency of CO_2 is not improved as depicted in Figure 16 (c).

2.2.8. Effect of $ScCO_2$ Immersion. Simulation studies indicate that the effect of $ScCO_2$ immersion on ESGR and CO_2 sequestration is negligible,[70] but different conclusions have been obtained in laboratory experiments.[15,68,71] It can be clearly observed that all values of S_{CO_2/CH_4} decreased to varying degrees after $ScCO_2$ immersion (Figure 17 (a)), signifying that $ScCO_2$ weakened the selective adsorption advantage of shale to CO_2 to a certain extent, and they indicated that the decrease in S_{CO_2/CH_4} is mainly related to the change in the pore structure of shale. As described in Figure 17 (b), it can be seen that some micropores and mesopores in shale were converted to macropores after $ScCO_2$ immersion.[72−75] Theoretically, CO_2 molecules can enter smaller pore structures compared with CH_4 molecules because the molecular diameter of CO_2 is smaller than that of CH_4. Therefore, the expansion of the pore structure in shale after $ScCO_2$ immersion will reduce the adsorption advantage of shale for CO_2, thus leading to a decrease in S_{CO_2/CH_4}.

In addition, the influence of changes in organic matter and the mineral composition of shale after $ScCO_2$ treatment on S_{CO_2/CH_4} cannot be ignored. Relevant studies[76,77] indicated that after CO_2 is dissolved in water, water molecules will react to form carbonic acid, reducing the pH value of the solution, extracting organic matter from shale, dissolving some

https://doi.org/10.1021/acsomega.4c08678
ACS Omega 2025, 10, 12756−12771

carbonates (calcite, dolomite) and clay minerals (illite, kaolinite, montmorillonite, etc.) in the shale, thus producing some secondary minerals (such as quartz, kaolinite, etc.), and finally resulting in an increase in the percentage content of quartz in shale (Figure 18). According to Figure 8 and Figure 18, it can be inferred that the decrease in the TOC content of shale after $ScCO_2$ treatment may result in a decrease in S_{CO_2/CH_4}.

3. IMPLICATIONS FOR SHALE GAS RECOVERY AND CO_2 GEOLOGICAL STORAGE

After CO_2 injection into shale reservoirs, the competitive adsorption of CO_2/CH_4 will affect the efficiency of shale gas recovery and the potential for CO_2 storage, and relevant on-site experiments have been conducted in recent years.[10,78] For example, the first field test of CO_2 injection in the United States was conducted in the Chattanooga shale reservoir in Morgan County, Tennessee[10] (Figure 19). About 500 tons of CO_2 was injected into the shale reservoir by engineering in 2 weeks, the well was sealed and soaked for four months. It is found that the shale gas recovery rate was improved, the recovery rate of shale gas after CO_2 injection was about 8 times higher than before injection, and the production life of the gas well was extended by 15 months.

In practical engineering, in order to maximize shale gas recovery and CO_2 storage, the appropriate injection gas and injection scheme should be selected according to the geological conditions of the shale reservoir. In addition, the interactions between $ScCO_2$ and water−rock systems will change the mineral composition and pore structure of shale, which will lead to changes in the adsorption behavior of shale on CO_2 and CH_4, thus affecting the adsorption and replacement effect of CO_2 on CH_4 (Figure 20). Therefore,

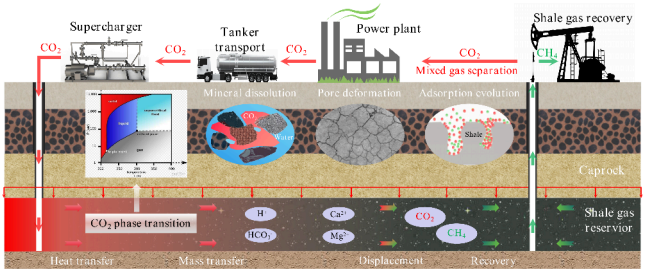

Figure 20. Schematic diagram of $ScCO_2$ enhanced shale gas exploitation and its geological storage integration.

after CO_2 is injected into shale reservoirs, the appropriate soaking time is also an important factor to be considered, which can be determined through a combination of experimental research and numerical simulation.

In addition, the assessment of the CO_2 storage potential after the depletion of shale gas reservoirs is also an important issue that needs to be addressed. Currently, scholars[79−82] have carried out a large number of studies on deep saline aquifers, depleted oil and gas fields, deep unminable coal beds, and shallow seas as CO_2 storage geological bodies and have denoted that the CO_2 storage potential of geological bodies is not only affected by geological conditions such as scale, burial depth, porosity, permeability but also closely related to technology, economy, policy measures, and other factors. The calculation of the storage capacity is a key task for evaluating the CO_2 storage potential of geologic bodies. According to the differences in the purpose of evaluation and the understanding levels of geologic bodies, a technology−economic resource pyramid model was proposed by relevant scholars[83] to characterize the potential of CO_2 geological storage (Figure 21). This model divides the potential of CO_2

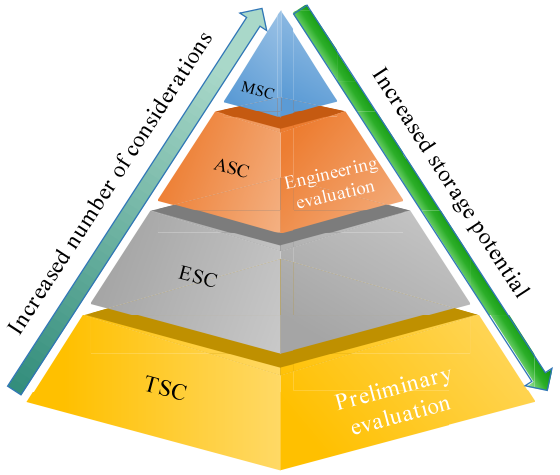

Figure 21. Pyramid model of the CO_2 geological storage capacity.

storage into four levels—theoretical storage capacity (TSC), effective storage capacity (ESC), actual storage capacity (ASC), and matching storage capacity (MSC)—and suggests that the initial assessment of the geological CO_2 storage potential should focus on TSC and ESC.

Previous studies[80,82,84,85] have denoted that there are great differences in the CO_2 sequestration mechanism among different sequestration geological bodies, and the evaluation methods of the CSLF (Carbon Sequestration Leaders Forum), US-DOE (United States Department of Energy), UE (European Union), RIPED&CUP evaluation method, novel evaluation method, and three parameters method synchronous storage calculation method were established (Table 2). Among them, the current mainstream methods mainly include the US-DOE and USGS methods based on volume balance theory,[84,86] the CSLF method based on material balance theory,[82] and the RIPED&CUP method based on the dissolution trapping mechanism.[87] In addition, it should be noted that the CO_2 storage capacity of the geological body is closely related to its TOC and micropore content. When the geological body has the characteristics of a shallow burial depth, abnormal pressure, and high temperature, it is difficult to reach the supercritical state after CO_2 injection, so it cannot be used as an ideal CO_2 storage site.[88] In general, there are significant differences in the CO_2 storage capacity calculated by different calculation models. Therefore, the combination of experimental and theoretical research methods should be used in practical engineering to comprehensively consider the potential impact of various factors.

4. CHALLENGES AND PERSPECTIVES

After CO_2 is injected into shale gas reservoirs, the composition and microstructure of shale are altered in the process of the $ScCO_2$−water−rock interaction, leading to variations in the adsorption behavior of CO_2, CH_4, and their mixed gases in shale, which affects the adsorption and displacement effect of CO_2 on residual CH_4. Currently, a large amount of research[15,92−94] has been carried out on the mineral

https://doi.org/10.1021/acsomega.4c08678
ACS Omega 2025, 10, 12756−12771

Table 2. Calculation Methods for CO_2 Storage Capacity

Measuring Methods	Mathematical model	Representative researchers
US-DOE-NETL method	$G_{CO_2} = VE_V[\rho_{CO_2}\phi E_\phi + \rho_{SCO_2}(1-\phi)E_{s(d)} \times E_{s(m)}]M = \rho_r(CO_2)\cdot Ah\varphi(1-S_{wi})\cdot BE$	Ma et al.[83]
CSLF	$M_t(CO_2) = \rho_r(CO_2)\cdot[R_f Ah\varphi(1-S_{wi}) - V_{iw}+V_{pw}]M_e(CO_2) = C_e M_t(CO_2)$	Bachu et al.[82]
USGS	$TA_{SR} = (R_{SV} + B_{SV})\rho_r(CO_2)$	Brennan et al.[89]
RIPED&CUP	$M_t(CO_2) = \frac{\rho_r(CO_2)}{10^9}[R_{fb}Ah\varphi(1-S_{wi}) - V_{iw} + V_{pw} + C_{ws}(Ah\varphi S_{wi} + V_{iw} - V_{pw}) + C_{os}(1-R_{fb})Ah\varphi(1-S_{wi})]M_e = C_e M_t$	Shen et al.[87]
Novel evaluation methods	$M(CO_2) = \sum_{i=1}^{n} Q_{og}\left[s - \frac{\rho_{ings}}{1000}(GOR - R_{si})\right]\sum_{i=1}^{n} X_i$	Rezk et al.[90]
Three-parameter calculation method of CSSP	$M(CO_2) = \sum_{i=1}^{n} Q_{og}\left[s_{CO_2/oil} - \frac{\rho_{ings}}{1000}(GOR - R_{si})\right]$	Wang et al.[91]

composition, microstructure, and adsorption characteristics of shale under $ScCO_2$−water−rock action, but the following problems still need to be studied further.

CO_2/CH_4 competitive adsorption is a key factor affecting shale gas recovery and CO_2 geological storage.[9,46] However, there are currently difficulties in conducting mixed gas experiments and complex calculation processes for adsorption capacity, which leads to relatively enormous errors in the current test results and poor consistency among numerous research conclusions. Accordingly, it is necessary to improve the mixed gas adsorption test equipment and optimize the calculation method of the adsorption amount, thus systematically carrying out an in-depth analysis of the influence mechanism of different factors on the competitive adsorption of mixed gas via mixed gas adsorption tests combined with molecular simulation technology, finally revealing the competitive adsorption mechanism of CO_2/CH_4 in shale reservoirs.

Both CO_2 and N_2 injection can improve shale gas recovery to a certain extent,[67,95] but how to reasonably select the CO_2/N_2 mixed injection ratio from the perspectives of safety and economy is an important issue that needs to be addressed in future research. There is a threshold for the influence of the gas injection rate on ESGR and CGS, which may be closely related to shale reservoir geological conditions, gas injection modes (continuous injection, segmented injection, or pulsed injection), injected gas properties, etc. Future studies should pay attention to the influence of these potential factors. The effects of $ScCO_2$ injection on the composition and microstructure of shale cannot be ignored, thus the potential influences of $ScCO_2$−water−rock interaction on ESGR and CGS need to be considered in the future simulation process by combining with laboratory test results. In addition, there are significant differences in the CO_2 storage capacity calculated by different CO_2 storage calculation models, hence various factors should be considered comprehensively and the calculation method of the CO_2 storage capacity should be carefully selected in practical engineering.

5. CONCLUSIONS

This study systematically expounds on the competitive adsorption process of CO_2 and CH_4 in shale, analyzes the influence mechanism of different factors on S_{CO_2/CH_4}, and discusses the potential influence of CO_2/CH_4 competitive adsorption on shale gas recovery and CO_2 geological storage. The main conclusions are as follows:

(1) S_{CO_2/CH_4} is generally proportional to TOC and inversely proportional to clay mineral content, which can be interpreted by the abundant high-energy adsorption sites in organic matter and the hydrophobicity of clay minerals. S_{CO_2/CH_4} decreases with increasing temperature while the effects of pressure and the proportion of mixed gas components on S_{CO_2/CH_4} are relatively complex, which are mainly related to the changes in the adsorption site of gas molecules and the interactions among gas molecules in shale. In addition, the variation of S_{CO_2/CH_4} with water content is controlled by the type of organic matter in shale and the molar ratio of mixed gas.

(2) The injection type (CO_2 or N_2), injection mode (continuous injection or pulse injection), and injection rate of gases exhibit significant effects on shale gas recovery and CO_2 geological storage, and the CO_2/N_2 mixed gas injection scheme is recommended in actual engineering projects.

(3) The $ScCO_2$−water−rock interaction can dissolve organic matter and minerals of shale, change the microscopic pore structure of shale, lead to changes in the adsorption behavior of CO_2 and CH_4 in shale, and affect the adsorption and replacement effects of CO_2 on CH_4 in shale during the soaking process. Therefore, the potential impact of $ScCO_2$ soaking on CO_2/CH_4 competitive adsorption in practical engineering cannot be ignored.

(4) Both CO_2 and N_2 injection can improve the recovery rate of shale gas to a certain extent, but the injection effects of the two schemes are significantly different. It is recommended to use a CO_2/N_2 mixed gas injection scheme in practical engineering. The effect of CO_2 pulse injection is obviously better than that of continuous injection, and a reasonable gas injection rate should be selected according to actual shale reservoir conditions.

(5) Significant differences existed in the CO_2 storage mechanism for different geological bodies, and the CO_2 storage capacity of a geological body is closely related to TOC and the micropore content while the geological body with a shallow burial depth, abnormal

https://doi.org/10.1021/acsomega.4c08678
ACS Omega 2025, 10, 12756−12771

pressure, and high temperature is not an ideal place for CO_2 sequestration.

AUTHOR INFORMATION

Corresponding Author

Chao Qin − *College of Resources and Environmental Engineering, Key Laboratory of Karst Georesources and Environment, Ministry of Education, Guizhou University, Guiyang 550025, China;* orcid.org/0009-0000-0789-6506; Phone: +86 18875208371; Email: qinchao5018@163.com

Authors

Mengyao Cao − *College of Resources and Environmental Engineering, Key Laboratory of Karst Georesources and Environment, Ministry of Education, Guizhou University, Guiyang 550025, China*

Yongdong Jiang − *State Key Laboratory of Coal Mine Disaster Dynamics and Control, Chongqing University, Chongqing 400044, China;* orcid.org/0000-0002-2839-9776

Peng Xia − *College of Resources and Environmental Engineering, Key Laboratory of Karst Georesources and Environment, Ministry of Education, Guizhou University, Guiyang 550025, China;* orcid.org/0009-0000-9342-0378

Ke Wang − *College of Resources and Environmental Engineering, Key Laboratory of Karst Georesources and Environment, Ministry of Education, Guizhou University, Guiyang 550025, China;* orcid.org/0000-0002-8294-2186

Complete contact information is available at: https://pubs.acs.org/10.1021/acsomega.4c08678

Notes

The authors declare no competing financial interest.

ACKNOWLEDGMENTS

The research presented here was supported by Guizhou Provincial Basic Research Program (Natural Science) (ZK[2022]099 and ZK[2024]026); Young Talent Introduction Program of GZU (no. (2021) 63); Basic Research Project of GZU (no. 2023)53); and Key Technologies and Engineering Tests of Shale Gas Benefit Development in Guizhou Province ([2022]ZD005).

REFERENCES

(1) Zhang, C.-Y.; Chai, X.-S.; Xiao, X.-M. A simple method for correcting for the presence of minor gases when determining the adsorbed methane content in shale. *Fuel* **2015**, *150*, 334−338.

(2) Zhang, F.; Damjanac, B.; Maxwell, S. Investigating Hydraulic Fracturing Complexity in Naturally Fractured Rock Masses Using Fully Coupled Multiscale Numerical Modeling. *Rock Mechanics and Rock Engineering* **2019**, *52* (12), 5137−5160.

(3) Zhang, X.; Lu, Y.; Tang, J.; Zhou, Z.; Liao, Y. Experimental study on fracture initiation and propagation in shale using supercritical carbon dioxide fracturing. *Fuel* **2017**, *190*, 370−378.

(4) Middleton, R. S.; Gupta, R.; Hyman, J. D.; Viswanathan, H. S. The shale gas revolution: Barriers, sustainability, and emerging opportunities. *Applied Energy* **2017**, *199*, 88−95.

(5) Yang, R.; Liu, X.; Yu, R.; Hu, Z.; Duan, X. Long short-term memory suggests a model for predicting shale gas production. *Applied Energy* **2022**, *322*, 119415.

(6) Liao, Q.; Zhou, J.; Xian, X.; Yang, K.; Zhang, C.; Dong, Z.; Yin, H. Competition adsorption of CO_2/CH_4 in shale: Implications for CO_2 sequestration with enhanced gas recovery. *Fuel* **2023**, *339*, 127400.

(7) Liu, B.; Qi, C.; Mai, T.; Zhang, J.; Zhan, K.; Zhang, Z.; He, J. Competitive adsorption and diffusion of CH_4/CO_2 binary mixture within shale organic nanochannels. *Journal of Natural Gas Science and Engineering* **2018**, *53*, 329−336.

(8) Wang, S.; Zhou, S.; Pan, Z.; Elsworth, D.; Yan, D.; Wang, H.; Liu, D.; Hu, Z. Response of pore network fractal dimensions and gas adsorption capacities of shales exposed to supercritical CO_2: Implications for CH_4 recovery and carbon sequestration. *Energy Reports* **2023**, *9*, 6461−6485.

(9) Liu, J.; Xie, L.; Elsworth, D.; Gan, Q. CO_2/CH_4 Competitive Adsorption in Shale: Implications for Enhancement in Gas Production and Reduction in Carbon Emissions. *Environ. Sci. Technol.* **2019**, *53* (15), 9328−9336.

(10) Louk, K.; Ripepi, N.; Luxbacher, K.; Gilliland, E.; Tang, X.; Keles, C.; Schlosser, C.; Diminick, E.; Keim, S.; Amante, J.; et al. Monitoring CO_2 storage and enhanced gas recovery in unconventional shale reservoirs: Results from the Morgan County, Tennessee injection test. *Journal of Natural Gas Science and Engineering* **2017**, *45*, 11−25.

(11) Klewiah, I.; Berawala, D. S.; Alexander Walker, H. C.; Andersen, P. Ø.; Nadeau, P. H. Review of experimental sorption studies of CO_2 and CH_4 in shales. *Journal of Natural Gas Science and Engineering* **2020**, *73*, 103045.

(12) Rani, S.; Padmanabhan, E.; Prusty, B. K. Review of gas adsorption in shales for enhanced methane recovery and CO_2 storage. *J. Pet. Sci. Eng.* **2019**, *175*, 634−643.

(13) Zhou, J.; Liu, M.; Xian, X.; Jiang, Y.; Liu, Q.; Wang, X. Measurements and modelling of CH_4 and CO_2 adsorption behaviors on shales: Implication for CO_2 enhanced shale gas recovery. *Fuel* **2019**, *251*, 293−306.

(14) Ke, H.; Jiren, T.; Helmut, M. Investigation of supercritical shale gas adsorption in shale based on the Ono-Kondo lattice model. *Journal of China Coal Society* **2021**, *46* (8), 2479−2487.

(15) Qin, C.; Jiang, Y.; Zhou, J.; Song, X.; Liu, Z.; Li, D.; Zhou, F.; Xie, Y.; Xie, C. Effect of supercritical CO_2 extraction on CO_2/CH_4 competitive adsorption in Yanchang shale. *Chemical Engineering Journal* **2021**, *412*, 128701.

(16) Wang, T.; Tian, S.; Li, G.; Sheng, M.; Ren, W.; Liu, Q.; Zhang, S. Molecular simulation of CO_2/CH_4 competitive adsorption on shale kerogen for CO_2 sequestration and enhanced gas recovery. *J. Phys. Chem. C* **2018**, *122* (30), 17009−17018.

(17) Jin, D.; Lu, X.; Zhang, M.; Wei, S.; Zhu, Q.; Shi, X.; Shao, Y.; Wang, W.; Guo, W. The adsorption behaviour of CH_4 on microporous carbons: effects of surface heterogeneity. *Phys. Chem. Chem. Phys.* **2014**, *16* (22), 11037.

(18) Zhang, H.; Cao, D. Molecular simulation of displacement of shale gas by carbon dioxide at different geological depths. *Chem. Eng. Sci.* **2016**, *156*, 121−127.

(19) Lee, T.; Bocquet, L.; Coasne, B. Activated desorption at heterogeneous interfaces and long-time kinetics of hydrocarbon recovery from nanoporous media. *Nat. Commun.* **2016**, *7* (1), DOI: 10.1038/ncomms11890.

(20) Adewumi Babatunde, K.; Mamo Negash, B.; Rashik Mojid, M.; Ahmed, T. Y.; Regassa Jufar, S. Molecular simulation study of CO_2/CH_4 adsorption on realistic heterogeneous shale surfaces. *Appl. Surf. Sci.* **2021**, *543*, 148789.

(21) Liu, Z.; Bai, B.; Wang, Y.; Ding, Z.; Li, J.; Qu, H.; Jia, Z. Experimental study of friction reducer effect on dynamic and isotherm of methane desorption on Longmaxi shale. *Fuel* **2021**, *288*, 119733.

(22) Lim, Y.-I.; Bhatia, S. K. Simulation of methane permeability in carbon slit pores. *J. Membr. Sci.* **2011**, *369* (1−2), 319−328.

(23) Cheng, H.; Lei, G. Multilayer graphene nanostructure separate CO_2/CH_4 mixture: Combining molecular simulations with ideal adsorbed solution theory. *Chem. Phys. Lett.* **2016**, *661*, 31−35.

(24) Ma, J.; Yao, M.; Yang, Y.; Zhang, X. Comprehensive review on stability and demulsification of unconventional heavy oil-water emulsions. *J. Mol. Liq.* **2022**, *350*, 118510.
(25) Zhang, S. H.; Tang, S. H.; Li, Z. C.; Pan, Z. J.; Liu, B. Competitive sorption and diffusion of methane and carbon dioxide mixture in Carboniferous-Permian anthracite of south Qinshui Basin, China. *Arabian Journal of Geosciences* **2020**, *13* (24), Article.
(26) Pan, Z.; Connell, L. D. Comparison of adsorption models in reservoir simulation of enhanced coalbed methane recovery and CO_2 sequestration in coal. *International Journal of Greenhouse Gas Control* **2009**, *3* (1), 77−89.
(27) Zhan, J.; Niu, Z.; Li, M.; Zhang, Y.; Ma, X.; Fan, C.; Wang, R.; Zendehboudi, S. Numerical Simulation and Modeling on CO_2 Sequestration Coupled with Enhanced Gas Recovery in Shale Gas Reservoirs. *Geofluids* **2021**, *2021*, 1−15.
(28) Siyu, L.; Guodong, Y.; Mian, H.; Shuguo, Y.; Xin, M.; Qi, B. Effects of artificial fracture parameters on CO_2 sequestration and CH_4 production in CO_2-ESGR. *Chemical Engineering of Oil &Gas* **2024**, *53* (2), 94−100.
(29) Shabani, B.; Vilcáez, J. A fast and robust TOUGH2 module to simulate geological CO_2 storage in saline aquifers. *Computers & Geosciences* **2018**, *111*, 58−66.
(30) Shuguo, Y.; Guodong, Y.; Tao, F.; Xin, M.; Wei, C.; Mian, H.; Tianqing, G. Effects of Physical Parameters of Shale on CO_2 Storage Capacity with Different Mechanisms. *Geological Journal of China Universities* **2023**, *29* (1), 37−46.
(31) Lee, H.-H.; Kim, H.-J.; Shi, Y.; Keffer, D.; Lee, C.-H. Competitive adsorption of CO_2/CH_4 mixture on dry and wet coal from subcritical to supercritical conditions. *Chemical Engineering Journal* **2013**, *230*, 93−101.
(32) Songhang, Z.; Shouren, Z.; Shuheng, T.; Di, X.; Bing, L. Adsorption and transport of methane and carbon dioxide mixture in anthracite. *Journal of China Coal Society* **2021**, *46* (2), 544−555.
(33) Luo, X.; Wang, S.; Wang, Z.; Jing, Z.; Lv, M.; Zhai, Z.; Han, T. Adsorption of methane, carbon dioxide and their binary mixtures on Jurassic shale from the Qaidam Basin in China. *International Journal of Coal Geology* **2015**, *150*−*151*, 210−223.
(34) Rongrong, Q. *Study on Multi-Component Competitive Adsorption Mechanism of Shale Gas*; China University of Petroleum, Beijing, 2019.
(35) Xie, W.; Wang, M.; Chen, S.; Vandeginste, V.; Yu, Z.; Wang, H. Effects of gas components, reservoir property and pore structure of shale gas reservoir on the competitive adsorption behavior of CO_2 and CH_4. *Energy* **2022**, *254*, 124242.
(36) Duan, S.; Gu, M.; Du, X.; Xian, X. Adsorption Equilibrium of CO_2 and CH_4 and Their Mixture on Sichuan Basin Shale. *Energy Fuels* **2016**, *30* (3), 2248−2256.
(37) Gu, M.; Xian, X.; Duan, S.; Du, X. Influences of the composition and pore structure of a shale on its selective adsorption of CO_2 over CH_4. *Journal of Natural Gas Science and Engineering* **2017**, *46*, 296−306.
(38) Du, X.; Cheng, Y.; Liu, Z.; Hou, Z.; Wu, T.; Lei, R.; Shu, C. Study on the adsorption of CH_4, CO_2 and various CH_4/CO_2 mixture gases on shale. *Alexandria Engineering Journal* **2020**, *59* (6), 5165−5178.
(39) Ortiz Cancino, O. P.; Pino Pérez, D.; Pozo, M.; Bessieres, D. Adsorption of pure CO_2 and a CO_2/CH_4 mixture on a black shale sample: Manometry and microcalorimetry measurements. *J. Pet. Sci. Eng.* **2017**, *159*, 307−313.
(40) Qi, R.; Ning, Z.; Wang, Q.; Zeng, Y.; Huang, L.; Zhang, S.; Du, H. Sorption of Methane, Carbon Dioxide, and Their Mixtures on Shales from Sichuan Basin, China. *Energy Fuels* **2018**, *32* (3), 2926−2940.
(41) Ma, Y.; Yue, C.; Li, S.; Xu, X.; Niu, Y. Study of CH_4 and CO_2 competitive adsorption on shale in Yibin, Sichuan Province of China. *Carbon Resources Conversion* **2019**, *2* (1), 35−42.
(42) Ma, X.; Guo, S. Comparative Study on Shale Characteristics of Different Sedimentary Microfacies of Late Permian Longtan Formation in Southwestern Guizhou, China. *Minerals* **2019**, *9* (1), 20.
(43) Wang, Q.; Huang, L. Molecular insight into competitive adsorption of methane and carbon dioxide in montmorillonite: Effect of clay structure and water content. *Fuel* **2019**, *239*, 32−43.
(44) Rezlerová, E.; Brennan, J. K.; Lísal, M. Methane and carbon dioxide in dual-porosity organic matter: Molecular simulations of adsorption and diffusion. *AIChE J.* **2021**, *67* (3), DOI: 10.1002/aic.16655.
(45) Tesson, S.; Firoozabadi, A. Methane Adsorption and Self-Diffusion in Shale Kerogen and Slit Nanopores by Molecular Simulations. *J. Phys. Chem. C* **2018**, *122* (41), 23528−23542.
(46) Huang, L.; Ning, Z.; Wang, Q.; Zhang, W.; Cheng, Z.; Wu, X.; Qin, H. Effect of organic type and moisture on CO_2/CH_4 competitive adsorption in kerogen with implications for CO_2 sequestration and enhanced CH_4 recovery. *Applied Energy* **2018**, *210*, 28−43.
(47) Sui, H.; Zhang, F.; Wang, Z.; Wang, D.; Wang, Y. Effect of Kerogen Maturity, Water Content for Carbon Dioxide, Methane, and Their Mixture Adsorption and Diffusion in Kerogen: A Computational Investigation. *Langmuir* **2020**, *36* (33), 9756−9769.
(48) Hu, X.; Deng, H.; Lu, C.; Tian, Y.; Jin, Z. Characterization of CO_2/CH_4 Competitive Adsorption in Various Clay Minerals in Relation to Shale Gas Recovery from Molecular Simulation. *Energy Fuels* **2019**, *33* (9), 8202−8214.
(49) Pan, B.; Gong, C.; Wang, X.; Li, Y.; Iglauer, S. The interfacial properties of clay-coated quartz at reservoir conditions. *Fuel* **2020**, *262*, 116461.
(50) Zhou, W.; Wang, H.; Yan, Y.; Liu, X. Adsorption mechanism of CO_2/CH_4 in kaolinite clay: Insight from molecular simulation. *Energy Fuels* **2019**, *33* (7), 6542−6551.
(51) Zhou, W.; Zhang, Z.; Wang, H.; Yan, Y.; Liu, X. Molecular insights into competitive adsorption of CO_2/CH_4 mixture in shale nanopores. *RSC Adv.* **2018**, *8* (59), 33939−33946.
(52) Qi, R.; Ning, Z.; Wang, Q.; Huang, L.; Wu, X.; Cheng, Z.; Zhang, W. Measurements and modeling of high-pressure adsorption of CH_4 and CO_2 on shales. *Fuel* **2019**, *242*, 728−743.
(53) Zhou, W.; Wang, H.; Yang, X.; Liu, X.; Yan, Y. Confinement effects and CO_2/CH_4 competitive adsorption in realistic shale kerogen nanopores. *Ind. Eng. Chem. Res.* **2020**, *59* (14), 6696−6706.
(54) Xie, W.; Wang, M.; Wang, H. Adsorption Characteristics of CH_4 and CO_2 in Shale at High Pressure and Temperature. *ACS Omega* **2021**, *6* (28), 18527−18536.
(55) Wang, S.; Javadpour, F.; Feng, Q. Fast mass transport of oil and supercritical carbon dioxide through organic nanopores in shale. *Fuel* **2016**, *181*, 741−758.
(56) Zeng, K.; Jiang, P.; Lun, Z.; Xu, R. Molecular Simulation of Carbon Dioxide and Methane Adsorption in Shale Organic Nanopores. *Energy Fuels* **2019**, *33* (3), 1785−1796.
(57) Pan, Z.; Ye, J.; Zhou, F.; Tan, Y.; Connell, L. D.; Fan, J. CO_2 storage in coal to enhance coalbed methane recovery: a review of field experiments in China. *International Geology Review* **2018**, *60* (5−6), 754−776.
(58) Bai, P. S. *Studies on Adsorption Behavior of CO_2 on Porous Solids near the Critical Temperature*. Tianjin University, 2003.
(59) Lu, T.; Zeng, K.; Jiang, P.; Zhou, B.; Xu, R. Competitive adsorption in CO_2 enhancing shale gas: Low-field NMR measurement combined with molecular simulation for selectivity and displacement efficiency model. *Chemical Engineering Journal* **2022**, *440*, 135865.
(60) Sun, H.; Zhao, H.; Qi, N.; Li, Y. Molecular insights into the enhanced shale gas recovery by Carbon Dioxide in Kerogen Slit-Nanopores. *J. Phys. Chem. C* **2017**, *121*, 10233.
(61) Huang, L.; Ning, Z.; Wang, Q.; Qi, R.; Zeng, Y.; Qin, H.; Ye, H.; Zhang, W. Molecular simulation of adsorption behaviors of methane, carbon dioxide and their mixtures on kerogen: Effect of kerogen maturity and moisture content. *Fuel* **2018**, *211*, 159−172.
(62) Jin, Z.; Firoozabadi, A. Effect of water on methane and carbon dioxide sorption in clay minerals by Monte Carlo simulations. *Fluid Phase Equilib.* **2014**, *382*, 10−20.
(63) Zhang, K.; Jiang, H.; Qin, G. Utilization of zeolite as a potential multi-functional proppant for CO_2 enhanced shale gas recovery and CO_2 sequestration: A molecular simulation study of the impact of

https://doi.org/10.1021/acsomega.4c08678
ACS Omega 2025, 10, 12756−12771

water on adsorption in zeolite and organic matter. *Fuel* **2021**, *292*, 120312.
(64) Sun, J.; Chen, C.; Hu, W.; Cui, J.; Jiang, L.; Liu, Y.; Zhao, Y.; Li, W.; Song, Y. Asymmetric competitive adsorption of CO_2/CH_4 binary mixture in shale matrix with heterogeneous surfaces. *Chemical Engineering Journal* **2021**, *422*, 130025.
(65) Li, Z.; Elsworth, D. Controls of CO_2−N_2 gas flood ratios on enhanced shale gas recovery and ultimate CO_2 sequestration. *J. Pet. Sci. Eng.* **2019**, *179*, 1037−1045.
(66) Li, L.; Huang, Z.; Duan, X.; Niu, H.; Zhan, S.; Yang, Z.; Fan, Z.; Zhang, T. Insights into Enhancing Shale Oil Recovery Postfracturing with CO_2 Huff and Puff and Elastic Depletion Development Strategies. *Energy Fuels* **2024**, *38* (5), 3997−4009.
(67) Ma, H.; Yang, Y.; Zhang, Y.; Li, Z.; Zhang, K.; Xue, Z.; Zhan, J.; Chen, Z. Optimized schemes of enhanced shale gas recovery by CO_2-N_2 mixtures associated with CO_2 sequestration. *Energy Conversion and Management* **2022**, *268*, 116062.
(68) Li, L.; Su, Y.; Hao, Y.; Zhan, S.; Lv, Y.; Zhao, Q.; Wang, H. A comparative study of CO_2 and N_2 huff-n-puff EOR performance in shale oil production. *J. Pet. Sci. Eng.* **2019**, *181*, 106174.
(69) Li, X.; Elsworth, D. Geomechanics of CO_2 enhanced shale gas recovery. *Journal of Natural Gas Science and Engineering* **2015**, *26*, 1607−1619.
(70) Lan, Y.; Yang, Z.; Wang, P.; Yan, Y.; Zhang, L.; Ran, J. A review of microscopic seepage mechanism for shale gas extracted by supercritical CO_2 flooding. *Fuel* **2019**, *238*, 412−424.
(71) Yin, H.; Zhou, J.; Jiang, Y.; Xian, X.; Liu, Q. Physical and structural changes in shale associated with supercritical CO_2 exposure. *Fuel* **2016**, *184*, 289−303.
(72) Meng, S.; Jin, X.; Tao, J.; Wang, X.; Zhang, C. Evolution Characteristics of Mechanical Properties under Supercritical Carbon Dioxide Treatment in Shale Reservoirs. *ACS Omega* **2021**, *6* (4), 2813−2823.
(73) Goodman, A.; Sanguinito, S.; Tkach, M.; Natesakhawat, S.; Kutchko, B.; Fazio, J.; Cvetic, P. Investigating the role of water on CO_2-Utica Shale interactions for carbon storage and shale gas extraction activities − Evidence for pore scale alterations. *Fuel* **2019**, *242*, 744−755.
(74) Zhou, J.; Yang, K.; Zhou, L.; Jiang, Y.; Xian, X.; Zhang, C.; Tian, S.; Fan, M.; Lu, Z. Microstructure and mechanical properties alterations in shale treated via CO_2/CO_2-water exposure. *J. Pet. Sci. Eng.* **2021**, *196*, 108088.
(75) Zhou, D.; Zhang, G.; Huang, Z.; Zhao, J.; Wang, L.; Qiu, R. Changes in microstructure and mechanical properties of shales exposed to supercritical CO_2 and brine. *International Journal of Rock Mechanics and Mining Sciences* **2022**, *160*, 105228.
(76) Qin, C.; Jiang, Y.; Luo, Y.; Zhou, J.; Liu, H.; Song, X.; Li, D.; Zhou, F.; Xie, Y. Effect of supercritical CO_2 saturation pressures and temperatures on the methane adsorption behaviours of Longmaxi shale. *Energy* **2020**, *206*, 118150.
(77) Jiang, Y.; Luo, Y.; Lu, Y.; Qin, C.; Liu, H. Effects of supercritical CO_2 treatment time, pressure, and temperature on microstructure of shale. *Energy* **2016**, *97*, 173−181.
(78) Du, X.-D.; Gu, M.; Duan, S.; Xian, X.-F. Investigation of CO_2−CH_4 Displacement and Transport in Shale for Enhanced Shale Gas Recovery and CO_2 Sequestration. *J. Energy Resour. Technol.* **2017**, *139* (1), DOI: 10.1115/1.4035148.
(79) Bachu, S.; Bonijoly, D.; Bradshaw, J.; Burruss, R.; Holloway, S.; Christensen, N. P.; Mathiassen, O. M. CO_2 storage capacity estimation: Methodology and gaps. *International Journal of Greenhouse Gas Control* **2007**, *1* (4), 430−443.
(80) Hang, Y.; Qi, L.; Bo, P. Research progress in evaluation of carbon storage potential based on CO_2 flooding technology. *Clean Coal Technology* **2021**, *27* (2), 107−116.
(81) Zhao, D. F.; Liao, X. W.; Yin, D. D. Evaluation of CO_2 enhanced oil recovery and sequestration potential in low permeability reservoirs, Yanchang Oilfield, China. *Journal of the Energy Institute* **2014**, *87* (4), 306−313.
(82) Bachu, S. Comparison Between Methodologies Recommended for Estimation of CO_2 Storage Capacity in Geological Media. *Carbon Sequestration Leadership Forum* **2008**.
(83) Ma, L.; Fauchille, A.-L.; Ansari, H.; Chandler, M.; Ashby, P.; Taylor, K.; Pini, R.; Lee, P. D. Linking multi-scale 3D microstructure to potential enhanced natural gas recovery and subsurface CO_2 storage for Bowland shale, UK. *Energy Environ. Sci.* **2021**, *14* (8), 4481−4498.
(84) Ting, L.; Xin, M.; Yujie, D.; Xiaolin, J.; Jie, F.; Chenglong, Z. Research status of CO_2 geological storage potential evaluation methods at home and abroad. *Geological Survey Of China* **2021**, *8* (4), 101−108.
(85) Jessen, K.; Kovscek, A. R.; Orr, F. M. Increasing CO_2 storage in oil recovery. *Energy Conversion and Management* **2005**, *46* (2), 293−311.
(86) Huang, L.; Zhou, W.; Xu, H.; Wang, L.; Zou, J.; Zhou, Q. Dynamic fluid states in organic-inorganic nanocomposite: Implications for shale gas recovery and CO_2 sequestration. *Chemical Engineering Journal* **2021**, *411*, 128423.
(87) Pingping, S.; Xinwei, L.; Qingjie, L. Methodology for estimation of CO_2 storage capacity in reservoirs. *Petroleum Exploration and Development* **2009**, *36*, 216−220.
(88) Strąpoć, D.; Mastalerz, M.; Schimmelmann, A.; Drobniak, A.; Hasenmueller, N. R. Geochemical constraints on the origin and volume of gas in the New Albany Shale (Devonian−Mississippian), eastern Illinois Basin. *AAPG Bulletin* **2010**, *94* (11), 1713−1740.
(89) Brennan, B. S. T.; Burruss, R. C.; Merrill, M. D.; Freeman, P. A.; Ruppert, L. F. A probabilistic assessment methodology for the evaluation of geologic carbon dioxide storage. *USGS*; 2010.
(90) Rezk, M. G.; Foroozesh, J.; Zivar, D.; Mumtaz, M. CO_2 storage potential during CO_2 enhanced oil recovery in sandstone reservoirs. *Journal of Natural Gas Science and Engineering* **2019**, *66*, 233−243.
(91) Gaofeng, W.; Shunxi, Q.; Chunxia, H.; Xiangyu, C. Calculation of Carbon Dioxide Simultaneous Sequestration Potential in Low Permeable Reservoirs. *Science Technology and Engineering* **2019**, *19*(27), 148−154
(92) Fatah, A.; Ben Mahmud, H.; Bennour, Z.; Gholami, R.; Hossain, M. The impact of supercritical CO_2 on the pore structure and storage capacity of shales. *Journal of Natural Gas Science and Engineering* **2022**, *98*, 104394.
(93) Ao, X.; Lu, Y.; Tang, J.; Chen, Y.; Li, H. Investigation on the physics structure and chemical properties of the shale treated by supercritical CO_2. *Journal of CO_2 Utilization* **2017**, *20*, 274−281.
(94) Bai, B.; Ni, H.-j.; Shi, X.; Guo, X.; Ding, L. The experimental investigation of effect of supercritical CO_2 immersion on mechanical properties and pore structure of shale. *Energy* **2021**, *228*, 120663.
(95) Du, X.; Gu, M.; Liu, Z.; Zhao, Y.; Sun, F.; Wu, T. Enhanced Shale Gas Recovery by the Injections of CO_2, N_2, and CO_2/N_2 Mixture Gases. *Energy Fuels* **2019**, *33* (6), 5091−5101.

https://doi.org/10.1021/acsomega.4c08678
ACS Omega 2025, 10, 12756−12771